SYNTHESIS AND INTERFACIAL CHARACTERIZATION OF Al-4.5wt%Cu/ZIRCON SAND/SILICON CARBIDE HYBRID COMPOSITE

Thesis submitted in partial fulfillment of the requirement for
The award of the degree of
Master of Technology
In
MATERIALS SCIENCE AND ENGINEERING

Submitted by

VISHAL SHARMA
Roll No.60602016

Under
the guidance of
Dr. Sanjeev Das

School of Physics & Material Sciences
Thapar University, Patiala
Patiala - 147001
June-2007

Dedicated to my Loving Parents

CERTIFICATE

This is to certify that Mr. VISHAL SHARMA, Roll No. 60602016 has worked on this thesis report as a partial fulfillment for award of the degree of MASTERS OF TECHNOLGY in Material Science and Engineering. I certify that the matter embodied in this report is of the candidate's own record and not submitted to any other university in any part or full form for the award of such kind of a degree.

(Dr. Sanjeev Das)
Supervisor
SPMS, Thapar University
Patiala

Countersigned by:

Dr.O.P.Pandey
(Prof. & Head)
School of Physics and Materials Science
Thapar University, Patiala

Dr. R.K.Sharma
Dean of academic Affairs
Thapar University
Patiala

ACKNOWLEDGEMENT

No matter how much enterprising and entrepreneurial one's thinking is, yet nobody can do everything all by himself without some help and guidance. It is inhumane if the concerned person's assistance goes without appreciation and thanks. My first and foremost offering of thanks goes to the architect who shaped my dreams into reality, my guide and mentor Dr. Sanjeev Das. Perseverance, exuberance, positive approaches are just some of the traits he imprinted on my personality. He steered me through his journey through his invaluable advice, positive criticism, stimulating discussion and consistent encouragement. His meticulous attention towards my proceedings, his devoted time and his ideas has enabled me to make the project a success. His faith in me has always made me more confident. It had been my privilege to work under his guidance.

My greatest thanks are to Dr. O.P.Pandey, Prof. and Head, School of Physics and Material Science, Thapar University, Patiala. He has been very helpful in improving. I am grateful to him for sharing his time and expertise. I would like to thank Dr. Kulvir Singh, Assistant Professor, School of Physics and Materials Science for his full motivation and appreciation to my work. My special thanks to P G Lab incharge Mr. Purushottam. His assistance and partnership were of great pleasure. His comments and views were very insightful and helpful. I would also like to thank Mr. Jant Singh, for providing all kind of assistance in PG Lab for creating a healthy research environment.

I would also like to give many thanks to Research Scholar Kamalpreet Kaur and Vishal Kumar for any kind of help and valuable suggestions whenever I needed out of their busy schedule. All the faculties, my friend Sanjay Kumar, and my colleagues at the Materials Science & Engineering program and the School of Physics and Material Sciences are acknowledged for providing me a friendly atmosphere and encouraging me throughout this research.

Vishal Sharma

Roll No.60602016

ABSTRACT

In the present investigation, Al-4.5wt%Cu/zircon sand/SiC hybrid composite has been synthesized by stir casting route by controlling various casting parameters. The as-cast samples were observed under optical and scanning electron microscope. Microstructural observations of the as-cast hybrid composite, shows uniform distribution of reinforcement particles and also good interfacial bonding between the particles and the matrix. Microhardness tester is employed to evaluate the interfacial bonding between the particles and the matrix by indenting the microhardness indenter on the particle with the varying load (100 gm, 200 gm, 300 gm) and time (10 sec, 15 sec, 20 sec and 25 sec). It has been concluded that by the variation in hardness at constant load varying time or at constant time varying load, the bond strength can be compared.

LIST OF TABLES

LIST OF FIGURES

LIST OF ABBREVIATIONS

SEM	Scanning electron microscopy
TEM	Transmission electron microscopy
Hv	Vicker's hardness
MMC	Metal Matrix Composites
PIR	Particle incorporation time
EDAX	Energy dispersive X-ray analysis
CTE	Coefficient of linear thermal expansion

CONTENTS

CHAPTER – 1

INTRODUCTION

In engineering designs, great interest is to search for new materials exhibiting good mechanical properties. For the development of such materials metal matrix composites (MMCs) have been proved to be one of the best selections for such materials [RSC 2003]. Composite materials are engineered materials made from two or more constituents material with significantly different physical and chemical properties and which remain separate and distinct on a macroscopic level with the finished structure. A metal matrix composite (MMC) is composite material with at least two constituent parts, one being a metal as matrix. The other material called as reinforcement may be a material such as a ceramic or organic compound . The reinforcement does not always serve a purely structural task (reinforcing the compound), but is also used to change physical properties such as wear resistance, friction coefficient, or thermal conductivity. For example, SiC particle introduced into the metal matrix is beneficial for mechanical strength. Zircon reinforced composite shows better wear resistance than alumina reinforced composite due to its superior particle–matrix bonding. [DAS 2007].

Matrix reinforced with two or more reinforcement types is known as hybrid composite. J. I. Song et al. successfully fabricated Al/Al_2O_3/C hybrid metal matrix composites by squeeze casting method. The wear resistance of hybrid composites of alumina and carbon fibers indicates more effectiveness than that in the composites reinforced with alumina fibers,
Jinhai Gu et al. synthesized 6061/Al/SiCp/Gr hybrid composite by spray atomization and deposition. The aim of this work is to improve mechanical properties of the material by introducing SiCp and Gr for damping property. Hence, a mixture of such different type and shape of reinforcements in an alloy matrix is of great interest for present researchers as it gives birth to a new generation of materials, which has a good combination of properties of different reinforcements.

Particulate reinforced metal matrix composites can be produced by two major routes: melt processing and powder metallurgy. Compared with powder metallurgy, melt processing has some important advantages, e.g., better matrix-particle bonding, easier control of metal

structure, simplicity and low cost of production. Among the variety of manufacturing processes available, stir casting is generally accepted as a particularly promising route. Its advantages lie in its simplicity, flexibility and applicability to large volume production. It is also attractive because, in principle, it allows a conventional metal processing route to be used, and hence minimizes the final cost of the product. This liquid metallurgy technique is the most economical of all the available routes for metal matrix composite production, and allows very large sized components to be fabricated [SUR 1997].

On the basis of all the above facts, in the present investigation Al-4.5wt%Cu/zircon sand/SiC hybrid composite is synthesized by stir casting route. The synthesized hybrid composite is then characterized using optical microscope, SEM with EDX, XRD studies. Microhardness values at each of the selected reinforcement particles are studied to compare the interfacial bonding between the particle–matrix interfaces for different reinforcements.

CHAPTER – 2

LITERATURE REVIEW

2.1 Metal matrix composite

A metal matrix composite (MMC) is composite material with at least two constituent parts, one being a metal. The other material may be a different metal or another material, such as a ceramic or organic compound. When at least three materials are present, it is called a hybrid composite. An MMC is complementary to a cermet.

MMCs are made by dispersing a reinforcing material into a metal matrix. The reinforcement surface can be coated to prevent a chemical reaction with the matrix. For example, carbon fibers are commonly used in aluminum matrix to synthesize composites containing low density and high strength. However, carbon reacts with aluminum to generate a brittle and water-soluble compound Al_4C_3 on the surface of the fiber. To prevent this reaction, the carbon fibers are coated with nickel or titanium boride.

2.2 Matrix

The matrix is the monolithic material into which the reinforcement is embedded, and is completely continuous. This means that there is a path through the matrix to any point in the material, unlike two materials sandwiched together. In structural applications, the matrix is usually a lighter metal such as aluminum, magnesium, or titanium, and provides a compliant support for the reinforcement. In high temperature applications, cobalt and cobalt-nickel alloy matrices are common.

2.2.1 Matrix materials and key composites

Numerous metals have been used as matrices. The most important have been aluminum, titanium, magnesium, and copper alloys and superalloys.

The most important MMC systems are:

- Aluminum matrix

    - Continuous fibers: boron, silicon carbide, alumina, graphite
    - Discontinuous fibers: alumina, alumina-silica
    - Whiskers: silicon carbide
    - Particulates: silicon carbide, boron carbide

- Magnesium matrix

    - Continuous fibers: graphite, alumina
    - Whiskers: silicon carbide
    - Particulates: silicon carbide, boron carbide

- Titanium matrix

    - Continuous fibers: silicon carbide, coated boron
    - Particulates: titanium carbide

- Copper matrix

    - Continuous fibers: graphite, silicon carbide
    - Wires: niobium-titanium, niobium-tin
    - Particulates: silicon carbide, boron carbide, titanium carbide.

- Superalloy matrices

    - Wires: tungsten

2.3 Reinforcement

The reinforcement material is embedded into the matrix. The reinforcement does not always serve a purely structural task (reinforcing the compound), but is also used to change physical properties such as wear resistance, friction coefficient, or thermal conductivity. The reinforcement can be either continuous, or discontinuous. Discontinuous MMCs can be isotropic, and can be worked with standard metalworking techniques, such as extrusion, forging or rolling. In addition, they may be machined using conventional techniques, but commonly would need the use of polycrystaline diamond tooling. Continuous reinforcement uses monofilament wires or fibers such as carbon fiber or silicon carbide. Because the fibers are embedded into the matrix in a certain direction, the result is an anisotropic structure in

which the alignment of the material affects its strength. One of the first MMCs used boron filament as reinforcement. Discontinuous reinforcement uses "whiskers", short fibers, or particles. The most common reinforcing materials in this category are alumina and silicon carbide.

2.4 Manufacturing and forming methods

MMC manufacturing can be broken into three types: solid, liquid, and vapor.

2.4.1 Solid state methods

- Powder blending and consolidation (powder metallurgy): Powdered metal and discontinuous reinforcement are mixed and then bonded through a process of compaction, degassing, and thermo-mechanical treatment (possibly via hot isostatic pressing (HIP) or extrusion).
- Foil diffusion bonding: Layers of metal foil are sandwiched with long fibers, and then pressed through to form a matrix.

2.4.2 Liquid state methods

- Electroplating / Electroforming: A solution containing metal ions loaded with reinforcing particles is co-deposited forming a composite material.
- Stir casting: Discontinuous reinforcement is stirred into molten metal, which is allowed to solidify.
- Squeeze casting: Molten metal is injected into a form with fibers preplaced inside it.
- Spray deposition: Molten metal is sprayed onto a continuous fiber substrate.
- Reactive processing: A chemical reaction occurs, with one of the reactants forming the matrix and the other the reinforcement.

2.4.2.1 Stir casting route

Stir casting set-up mainly consists a furnace and a stirring assembly (Fig. 2.1). In general, the solidification synthesis of metal matrix composites involves producing a melt of the selected matrix material followed by the introduction of a reinforcement material into the melt, obtaining a suitable dispersion. The next step is the solidification of the melt containing

suspended dispersoids under selected conditions to obtain the desired distribution of the dispersed phase in the cast matrix.

In preparing metal matrix composites by the stir casting method, there are several factors that need considerable attention, including

1. The difficulty in achieving a uniform distribution of the reinforcement material.
2. Wettability between the two main substances.
3. Porosity in the cast metal matrix composites.
4. Chemical reactions between the reinforcement material and the matrix alloy.

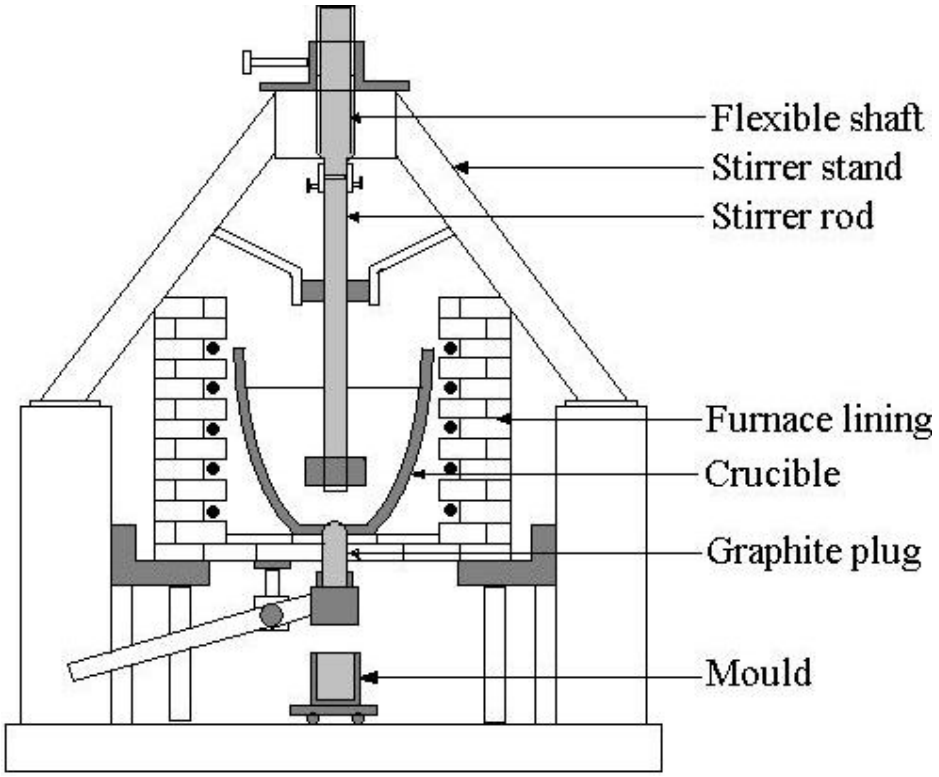

Fig.2.1 Stir casting process [BAN 1983]

In order to achieve the optimum properties of the metal matrix composite, the distribution of the reinforcement material in the matrix alloy must be uniform, and the wettability or bonding between these substances should be optimized. The porosity levels need to be minimized, and chemical reactions between the reinforcement materials and the matrix alloy must be avoided.

2.4.3 Vapor deposition

- Physical vapor deposition: The fiber is passed through a thick cloud of vaporized metal, coating it.

2.4.4 In situ fabrication technique

- Controlled unidirectional solidification of a eutectic alloy can result in a two-phase microstructure with one of the phases, present in lamellar or fiber form, distributed in the matrix.

2.5 Advantages of MMCs

Compared to monolithic metals, MMCs have:

- Higher strength-to-density ratios
- Higher stiffness-to-density ratios
- Better fatigue resistance
- Better elevated temperature properties
    - -- Higher strength
    - -- Lower creep rate

The advantages of MMCs over polymer matrix composites are:

- Higher temperature capability
- Fire resistance
- Higher transverse stiffness and strength
- No moisture absorption
- Higher electrical and thermal conductivities
- Better radiation resistance.

2.6 Disadvantages of MMCs

Some of the disadvantages of MMCs compared to monolithic metals and polymer matrix composites are:

- Higher cost of some material systems
- Relatively immature technology
- Complex fabrication methods for fiber-reinforced systems (except for casting)
- Limited service experience

2.7 Applications of MMCs

- Carbide drills are often made from a tough cobalt matrix with hard tungsten carbide particles inside.
- Some tank armors may be made from metal matrix composites, probably steel reinforced with boron nitride. Boron nitride is a good reinforcement for steel because it is very stiff and it does not dissolve in molten steel.
- Some automotive disc brakes use MMCs. Early Lotus Elise models used Aluminum MMC rotors, but they have less than optimal heat properties and Lotus has since switched back to cast-iron. Modern high-performance sport cars, such as those built by Porsche, use rotors made of carbon fiber within a silicon carbide matrix because of its high specific heat and thermal conductivity. 3M sells a preformed aluminum matrix insert for strengthening cast aluminum disc brake calipers allowing them to weigh as much as 50% less while increasing stiffness. 3M have also used alumina preforms for AMC pushrods.
- The F-16 Fighting Falcon uses monofilament silicon carbide fibres in a titanium matrix for a structural component of the jet's landing gear.
- Specialized Bicycles have used aluminium MMC compounds for their top of the range bicycle frames for several years.

In comparison with conventional polymer matrix composites, MMCs are resistant to fire, can operate in wider range of temperatures, do not absorb moisture, have better electrical and thermal conductivity, are resistant to radiation, and do not display outgassing. On the other hand, MMCs tend to be more expensive, the fiber-reinforced materials may be difficult to fabricate, and the available experience in use is limited.

2.8 Aluminum metal matrix composite

Aluminum metal matrix composites (Al MMCs) are materials in which reinforcement, typically a ceramic-based material, is added with the purpose of improving the materials

properties. When these reinforcements are combined with an aluminum matrix, the resulting material experiences significant increase in elastic modulus, wear resistance, strength and fatigue resistance. In addition, the coefficient of thermal expansion of aluminum is reduced by the addition of the reinforcement, while the material retains the high thermal conductivity and low density, characteristics of the aluminum alloy. These types of property changes, not generally possible through conventional alloying methods, have been the source of the excitement about the aluminum composites. The physical and mechanical properties of aluminum–based metal matrix composites have made them attractive materials for automotive and aerospace applications [SRI 1991] [TDP1998].

Properties of AL-MMCs are

a) High thermal conductivity
b) Low thermal expansion
c) Low relative density as compared to cast iron

2.9 Classification of aluminum metal-matrix composites

(a) Continuous fibers,
(b) Whiskers/discontinuous fibers
(c) Particulates.

The main reasons for adding reinforcements to aluminum alloys are to increase the strength, stiffness or wear resistance but this is usually achieved at the expense of other properties such as ductility.

The desirable properties of the reinforcements include:
1. High strength
2. High modulus
3. Ease of fabrication and low cost
4. Good chemical stability
5. Density and distribution
6. The thermal mismatch strain between reinforcement and the matrix.

2.9.1 Continuous fibers reinforced composite

The continuous fiber reinforced Al MMCs offer the best combination of strength and stiffness. However, the cost of these systems is very high, mainly because of the high costs of the continuous fibers and of the production [JOH 1987].

These materials are mainly of interest for aerospace or military industries, where weight savings and very specific properties are of great importance than material cost. Among the attractive properties of these materials the most important one is the elevated temperature strength. The possibility of mechanical working on these materials is small, and they are hardly recyclable.

2.9.2 Whiskers/discontinuous fibers reinforced composite

The whisker based composites are more costly than the particulate based ones, but offer higher strength in general [MOH 1988].

Compared to discontinuous reinforcements, such as polycrystalline flakes, particulates or chopped fibers, single crystal whiskers usually have a much greater tensile strength and are generally used to produce the highest strength discontinuously reinforced MMCs. It is easier to recycle these materials compared to the continuous fiber reinforced material when the correct matrix and reinforcement combination is selected.

2.9.3 Particulate reinforced composites

Particulate–reinforced Al MMCs are of particular interest due to their ease of fabrication, lower costs, and isotropic properties. However, the improvement in strength does not seem to be high and the strain to failure and fracture are low compared to the matrix material [JOH 1987]. The particulate reinforced Al MMCs are easier to recycle than the fiber reinforced ones provided that an appropriate matrix and particulate reinforcement combination is selected.

Overall strength of such particle- reinforced MMCs depends on size of the particles, the interparticle spacing, volume fraction of the particles, and the nature of matrix and reinforcement interface. Matrix properties including the work hardening coefficient, which improves the effectiveness of the reinforcement constraint, are also important.

Table 2.1 Properties of the ceramic particulate reinforcements available [GEI 1989] [RAC 1988] [ENG 1966].

Particulate Type	Density (g/cm^3)	Melting point (°C)	Modulus (GPa)	Coeff. of thermal expansion
BORIDES				
CrB_2	5.10	2100	-	7.5
MoB	8.65	2180	-	-
TiB_2	4.50	2800	515-574	7.8
ZrB_2	6.20	3200	-	5.9
CARBIDES			-	
B_4C	2.51	2350	450	4.5
CrC	7.00	3660	370	11
SiC	3.21	2690	450	4.5
TiC	4.95	3000	460	7.6
WC	15.50	2800	700	4.9
ZrC	6.75	3500	350	6.6
NITRIDES				
AlN	3.30	2200	320	5.5
BN	3.48	2500	195	7.5
Si_3N_4	3.60	1750	300	3.7
TiN	5.50	2900	-	9.4
ZrN	7.30	3000	-	7.0
OXIDES				
Al_2O_3	3.97	2015	380	8.0
BeO	3.06	2500	380	10.3
MgO	3.75	2620	275	13.0
SiO_2	2.65	1610	110	0.55
ThO_2	9.9	3200	240	104
TiO_2	4.26	1800	88	6.8
Y_2O_3	5.01	2375	-	9.3
ZrO_2	6.27	2500	185	8.0

2.10 Zircon Sand as reinforcement

Zircon sand consists of mostly zirconium silicate ($ZrSiO_4$) and some hafnium in addition to some rare earth elements, titanium minerals (Rutile, Ilmenite), monazite, etc. Zircon is used chiefly for facing on foundry moulds to increase the resistance against metal penetration. Milled zircon is used in refractory paint for coating the outside of moulds.
Zircon sand deposits have been found in abundance near Indian coastal regions of Kerala, Tamil Nadu and Orissa. Zircon was found to be a promising candidate as reinforcement material for aluminum, zinc and lead based composites

2.10.1 Advantages of using Zircon Sand as reinforcement

1. High hardness,
2. High modulus of elasticity,
3. High temperature resistance (melting point of 2500^{o}C),
4. Acid corrosion resistance and excellent thermal stability.

The last property is important since fabrication processes require drastic changes in temperature and large volumetric changes due to phase transformations can cause debonding at the interface. Furthermore, zircon possesses a very low thermal expansion coefficient compared to most other ceramic oxides. Therefore, a change in temperature would not give rise to very high thermal stresses within zircon particles.

Zircon particles can be incorporated to aluminum silicon alloy matrix by stir casting route and the dispersed amount can be further increased by the addition of magnesium in the melt [BAN 1983]. Fractography studies also confirmed that good bonding of zircon particles in aluminum and zinc aluminum alloys [BAN 1983] [SHA 1999].

Wear resistance properties of Al–4.5 wt%Cu alloy improve significantly after addition of alumina and zircon particles. Zircon reinforced composite shows better wear resistance than alumina reinforced composite due to its superior particle–matrix bonding. (DAS 2007)

Table 2.2: Properties of Zircon sand

Properties	Zircon Sand
M.P. (°C)	2500
Limit of application (°C)	1870
Hardness (Moh's Scale)	7.5
Density (g/cm^3)	4.5-4.7
Linear coeff. of expansion (10^{-6} K)	4.5
Fracture toughness ($MPa\text{-}m^{1/2}$)	5
Crystal structure	Tetragonal

2.11 Silicon Carbide as reinforcement

Silicon Carbide is the only chemical compound of carbon and silicon. It was originally produced by a high temperature electro-chemical reaction of sand and carbon. Silicon carbide is an excellent abrasive and has been produced and made into grinding wheels and other abrasive products for over one hundred years. Today the material has been developed into a high quality technical grade ceramic with very good mechanical properties. It is used in abrasives, refractories, ceramics, and numerous high-performance applications. The material can also be made an electrical conductor and has applications in resistance heating, flame igniters and electronic components. Silicon carbide is composed of tetrahedra of carbon and silicon atoms with strong bonds in the crystal lattice. This produces a very hard and strong material. The high thermal conductivity coupled with low thermal expansion and high strength give this material exceptional thermal shock resistant qualities. Silicon carbide ceramics with little or no grain boundary impurities maintain their strength to very high temperatures, approaching 1600°C with no strength loss.

2.11.1 Key Properties

- Low density
- High strength

- Low thermal expansion
- High thermal conductivity
- High hardness
- High elastic modulus
- Excellent thermal shock resistance
- Superior chemical inertness

SiC particles were more effective than Al_2O_3 particles for the improvement of wear resistance of Al matrix composites due to the high hardness. [HOS 1982]

Lee et.al also stated better wear resistance of SiC reinforced composites than that of Al_2O_3 reinforced composites. [LEE 1992]

An increase in the weight percentage of SiC particulates along the deposition direction led to a progressive increase in the porosity levels and matrix hardness for Al/SiCp and Al–Cu/SiCp. [NAI 2003]

Table 2.3: Properties of Silicon Carbide

Properties	Silicon carbide
M.P. (°C)	2200-2700
Limit of application (°C)	1400-1700
Hardness (Moh's Scale)	9
Density (g/cm^3)	3.2
Linear coeff. of expansion ($10^{-6}K$)	4.5
Fracture toughness ($MPa\text{-}m^{1/2}$)	4.6
Crystal structure	hexagonal

There are several literatures available for aluminium metal-matrix composites and they are as follows:

J. N. Wei et al. investigated the effect of macroscopic graphite (Gr) particulates on the damping behavior of commercially pure aluminum (Al). Macroscopic graphite particulate-reinforced commercially pure aluminum metal matrix composites (MMCs) were prepared by pressure infiltration process. The damping characterization was conducted on a multifunction internal friction apparatus (MFIFA). The internal friction (IF), as well as the relative dynamic modulus, was measured at frequencies of 0.5, 1.0 and 3.0 Hz over the temperature range of 25–400 °C. The microstructural analysis was performed using transmission electron microscopy (TEM). The damping capacity of the Al/Gr MMCs, with three different volume fractions of macroscopic graphite reinforcements, was compared with that of unreinforced commercially pure aluminum specimens. The damping capacity of the materials is shown to increase with increasing volume fraction of macroscopic graphite particulates. [WEI 2002]

Natrajan et al. studied the wear behavior of aluminium metal matrix composite (Al MMC) sliding against automobile friction material has been compared with the conventional grey cast iron. The grey cast iron disc has been machined from a brake drum of a commercial passenger car. The Al MMC disc has been manufactured by stir casting technique using A356 aluminium alloy and 25% silicon carbide particles and machined to the required size.

The friction and the wear behaviour of Al MMC, grey cast iron and the semi metallic brake shoe lining have been investigated at different sliding velocities, loads and sliding distances. The worn surfaces and sub-surface regions of MMC, the cast iron and the lining have been analysed using optical micrographs. The present investigation shows that the MMCs have considerable higher wear resistance than conventional grey cast iron while sliding against automobile friction material under identical conditions. A gradual reduction of friction coefficient with increase of applied load is observed for both cast iron and Al MMC materials. However, in all the tests it is observed that the friction coefficient of Al MMC is 25% more than the cast iron while sliding under identical conditions. The wear of the lining material has been observed more when sliding against MMC disc because of the ploughing of the lining material by the silicon carbide particles. [NAT 2006]

Olivier et al. studied the mechanical properties of high volume fraction SiC-particle reinforced Al-based metal matrix composites (MMCs) produced by means of pressurized liquid metal infiltration (squeeze casting) are shown to be triggered by matrix alloying and heat treatment procedures. It is distinguished between the effect of those alloying elements that only act on matrix strengthening, leaving the interface unaffected, and those alloying elements that interact with both (i.e. Mg). Among the first category a further sub-division is made between pure solid solution and precipitation hardening elements (i.e. Zn and Cu, ZnMg, respectively). In particular, this study addresses the effect of alloying and age hardening for AlCu3 and AlZn6Mg1 as well as the specific role of Mg additions to Al/SiC MMCs on interface microstructure formation, mechanical properties and fracture mode. For instance, it is shown that single additions of Mg catalyse the formation of Al4C3 whereas additions of Cu as well as (Zn + Mg) provide opportunities to enhance the composites' strength [OLI 2006]

Ferhat Gul & Mehmet Acilar investigated the effect of the reinforcement volume fraction on the dry sliding wear behaviour of Al–10Si/SiCp composites produced by vacuum infiltration technique was investigated. 0–40 vol% SiCp-reinforced composites were produced in the experimental study. In the infiltration process, an Al–10Si alloy was infiltrated into the compact of SiCp, Al and Mg powders inside the steel tubes. Sliding wear tests were carried out under the normal loads. Worn test specimens were examined by a scanning electron microscope (SEM) and energy dispersive X-ray analysis (EDAX) and wear mechanisms were determined. Tests were also carried out on the unreinforced matrix material. The MMCs exhibited excellent wear resistance compared with the unreinforced matrix. The volumetric wear rate increased with increasing applied load while it decreased with increasing volume fraction of the SiCp. The results showed that the wear mechanism was oxidation at low load levels and adhesion and delamination at high load levels in the composite having low volume fraction of reinforcement. [FER 2004]

T. Huber et al. studied the thermal expansion behaviour of different SiC particulate reinforced aluminium-matrix composites is investigated up to 500^0C using a thermal mechanical analysis

equipment. The aim is to explain abnormalities in the thermal expansion behaviour of 70 vol% SiC particulate reinforced aluminium-matrix composites (Al/SiC) used as base plate material for high power electronic modules. Composites with different SiC contents (10, 20, 55, 70 vol%), various matrix-alloy compositions (Al99.5, A356, A359), and different fabrication routes are investigated. The instantaneous coefficient of linear thermal expansion (CTE) as a function of temperature is compared with predictions from thermo-elastic models according to Schapery and Turner using the expansion data determined for the ingredients. The expansion behaviour is correlated to the microstructure, the deformation of the matrix, and the internal stress conditions. The temperature dependence of the solubility of Si in Al influences the CTE of Al–Si matrix alloys significantly. Composites with isolated ceramic particles (10–55 vol%) show similar thermal behaviour as the matrix alloy just reduced by the volume fraction of SiC-particles.
The CTE of highly reinforced Al/SiC(>55 vol% SiC), where the reinforcement is interconnected, drops above 250^0C. Such anomalies in the CTE are explained qualitatively by visco-plastic matrix deformations and changing void volume fractions. Although the matrix deforms non-elastic, the effects are reversible during reproduced thermal cycling. [**HUB 2006]**

2.12 Hybrid composites

Matrix reinforced with two or more reinforcement types are known as hybrid composite. The physical, mechanical and tribological properties of metal matrix composites depend upon the type and shape of reinforcement. For example, Hosking et al. reported that, SiC particles were more effective than Al_2O_3 particles for the improvement of wear resistance of Al matrix composites due to the high hardness [HOS 1982]. Where as continuous and discontinuous fibers reinforced composite have high tensile strength compared to particulate reinforced composites. Hence, a mixture of such different type and shape of reinforcements in an alloy matrix is of great interest for present researchers as it gives birth to a new generation of materials, which has a good combination of properties of different reinforcements. The hybrid materials are synthesized by the following routes:

1. Spray atomization and deposition process
2. Liquid pressure infiltration technique

3. Squeeze casting process

As these materials are one of the new varieties of material, limited work has been reported by the researchers and scientists.

R.K.Uyyuru et al. studied tribological behavior of Al-Si-SiCp composite / automobile brake pad system under dry sliding conditions by using discs of Al-MMCs of different formulations .Al-MMC s used in the study are reinforced with angular SiC particles of different size range and of different volume fractions. Friction and wear behavior have been studied against automobile brake pads.

Results of the study show:

- ✓ Both the wear rate and friction coefficient vary with the applied normal load and / or sliding speed are of different nature.
- ✓ Applied normal is most important parameter on wear performance .Influence of speed and concentration of abrasives on the other hand seemed to be composition dependent. when the SiCp reinforcement in the matrix has wide range distribution , wear rate and friction coefficient are found to be higher compared with matrix containing mono size reinforcement.
- ✓ Tribolayer formed during wear can act as a protective layer for the matrix material. Thus tribolayer can have significant role in wear behavior of tribological couple made of Al-Si-SiCp composite. **[RKU 2007]**

J. I. Song et al. successfully fabricated Al/Al_2O_3/C hybrid metal matrix composites by squeeze casting method. Optimum processing conditions for squeeze casting were obtained in order to achieve a uniform distribution of reinforcements and good bonding. Tensile strength and elongation of Al/Al_2O_3/C composites decrease owing to the increasing amount of added carbon fiber. On the contrary, elastic modulus of Al/Al_2O_3/C composites gets slightly increases compared with that of the unreinforced matrix alloy. The wear resistance of Al/Al_2O_3, and Al/Al_2O_3/C composites is remarkably improved by the addition of reinforcements compared to

matrix alloy. And in particular, wear behavior of $Al/Al_2O_3/C$ composites is improved by 20-30% more than that of Al/Al_2O_3 composites. The major wear mechanism of Al/Al obtained in order to achieve a uniform distribution of reinforcements and good bonding. Tensile strength and elongation of $Al/Al_2O_3/C$ composites decrease owing to the increasing amount of added carbon fiber. On the contrary, elastic modulus of $Al/Al_2O_3/C$ composites gets slightly increases compared with that of the unreinforced matrix alloy. The wear resistance of Al/Al_2O_3, and $Al/Al_2O_3/C$ composites is remarkably improved by the addition of reinforcements compared to matrix alloy. And in particular, wear behavior of $Al/Al_2O_3/C$ composites is the abrasive wear without accompanying the surface groove at intermediate sliding speed. The wear resistance of hybrid composites of alumina and carbon fibers indicates more effectiveness than that in the composites reinforced with alumina fibers. [SON 95]

Jinhai Gu et al. synthesized 6061/Al/SiCp/Gr hybrid composite by spray atomization and deposition. The aim of this work is to improve mechanical properties of the material by introducing SiCp and Gr for damping property. The results shows that internal friction spectra of samples exhibit internal fiction peak versus temperature at about 150^0C.The peak temperature increases with increasing frequencies It has been found that the strength of the magnesium matrix composites has been improved significantly at the expense of its damping capacity compared with that of pure magnesium. Moreover, the two damping peaks in the relaxation model have been reported in this paper. **[**JIN 2004**]**

Hui-Hui Fu et al. investigated the wear properties of Saffil/Al, Saffil/Al_2O_3/Al and Saffil/SiC/Al hybrid metal matrix composites (MMCs) fabricated by squeeze casting method. Wear tests have been carried out on a pin-on-disk friction and wear tester under both dry and lubricated conditions. The wear properties of the three composites are evaluated in many respects. The effects of Saffil fibers, Al_2O_3 particles and SiC particles on the wear behavior of the composites are elucidated. Under dry sliding condition, Saffil/SiC/Al shows the best wear resistance under high temperature and high load, while the wear resistances of Saffil/Al and Saffil/Al_2O_3/Al are quite similar. Under dry sliding condition, the dominant wear mechanism is abrasive wear under mild load and at room temperature, and the dominant wear mechanism changes to adhesive wear

as load or temperature increases. Compared with the dry sliding condition, all three composites show excellent wear resistance when lubricated by liquid paraffin. Under lubricated condition, Saffil/Al shows the best wear resistance among them, and its COF value is the smallest. The dominant wear mechanism of the composites under lubricated condition is microploughing, but microcracking also occurs to a certain extents. **[**HUI 2004**]**

Hayrettin Ahlatci et al. studied dry sliding metal–metal and metal–abrasive wear behaviors of the aluminum matrix hybrid composites produced by pressure infiltration technique . The composites were reinforced with 37 vol.% Al_2O_3 and 25 vol.% SiC particles and contained up to 8 wt% Mg in their matrixes. While matrix hardness and compression strength increases , amount of porosity and impact toughness decrease with increasing Mg content of the matrix. Metal–metal and metal–abrasive wear tests reveal that wear resistance of the composites increases with increasing Mg addition. Abrasion resistance of the hybrid composites decreases with increasing test temperature. When compared to the pure Al matrix hybrid composite Al–Mg alloy matrix hybrid composites exhibits abrupt increase in abrasion rate above 200°C. **[HAY 2006]**

Jinhai Gu et al. investigated the Mechanical properties and damping capacity of (SiCp + $Al_2O_3{\cdot}SiO_{2f}$)/Mg hybrid metal matrix composite fabricated by by the liquid pressure infiltration technique of fiber-particulate preform. At first, the SiCp and $Al_2O_3{\cdot}SiO_{2f}$ were mixed in a wet process and dispersed. Then, the preform was preheated and infiltrated by the magnesium melt under pressure of argon gas in the infiltration furnace. Finally, the composites were extruded into rods at 350 ◦C and the specimens for tensile and damping tests were cut from the rods. All the specimens were annealed at 350 ◦C for 1 h and then furnace cooled to room temperature before test. In the present work, the mechanical properties and damping capacity of (SiCp + $Al_2O_3{\cdot}SiO_{2f}$)/Mg hybrid MMCs were investigated. The following results were obtained:

(1) The introduction of reinforcement improved the strength of pure magnesium but decreased its plasticity. The tensile strength of the two composites with 8 and 18 vol. % reinforcements are increased by about 110 and 170%, respectively, compared with pure magnesium.

(2) The damping capacity of the Mg matrix composites is much lower than that of pure Mg. Dislocation damping and interface damping is the main damping mechanisms in Mg and its composites. **[**JIN 2004 x**]**

J.Zhang ,R.J.Perez, E.J.Lavernia, studied the effect of SiC and graphite (Gr) particulates on the resultant damping behavior of 606l AI metal matrix composites (MMCs) and investigated in an effort to develop a high damping material. The MMCs were processed by a spray atomization and deposition technique and the damping characterization was conducted on a dynamic mechanical thermal analyzer. The damping capacity, as well as the dynamic modulus, was measured at frequencies of 0.1, 1, 10 and 30 Hz over a 30 to 250°C temperature range. The microstructural analysis was performed using scanning electron microscopy, optical microscopy and image analysis. The damping capacity of the 6061 A1/SiC and 6061 A1/Gr MMCs, with two different volume fractions of reinforcements, were compared with that of as-received 6061-T6AI and spray deposited 6061 AI. It was shown that the damping capacity of 6061 AI could be significantly improved by the addition of either SiC or graphite particulates through spray deposition processing. Finally, the operative damping mechanisms were discussed in light of the data obtained from characterization of microstructure and damping capacity.

The spray deposited 6061 A1/Gr and 6061 A1/SiC MMCs were found to exhibit significant damping gains when compared to as-received 606 l-T6 A1 alloy both at ambient temperatures and at elevated temperatures. Damping capacity of the MMCs was noted to depend on volume fraction of graphite reinforcement but was relatively independent of volume fraction of SiC particulates. The 6061 A1/Gr MMCs exhibited a much higher damping capacity than that of the 6061 A1/SiC MMCs at temperatures below 200°C and have comparable damping capacity to the 6061 A1/SiC MMCs at 250°C. The damping of 6061 A1/Gr MMCs results primarily from the dislocations, reinforcement/matrix interface and the graphite particulates, while the damping capacity of 6061 A1/SiC MMCs is attributed to dislocations and interfaces. At elevated temperatures, interface damping plays a dominant role in the overall damping of the MMCs studied herein. [JHA 94]

Manchang Gui and Suk Bong Kang investigated the production of aluminum matrix composite coatings containing SiC_p, as well as aluminum hybrid composite coatings containing

SiC and graphite particles was explored by plasma spraying of premixed powders onto a solid aluminum alloy substrate. In both Al+SiC and Al+SiC+Gr composite coatings, SiC particles have a quite uniform distribution, while the distribution of graphite particles is inhomogeneous. No visible interval between the coating and the substrate can be found, which proved a good compatibility and intimate bonding between them. And no interfacial reaction products can be seen. [**MAN 2001]**

S. Wilson and A. T. Alpas studied the effect of ceramic particulate and graphite additions on the high temperature dry sliding wear resistance of two Al alloys was studied. The experiments were performed using a ring-on-flat sliding contact configuration against hardened SAE 52100 bearing steel counterfaces on an apparatus built for testing at controlled temperatures. Conditions were selected such that the materials in contact were kept in an isothermal atmosphere and the generation of frictional heat was minimized by the use of a low load (11.55 N) and sliding speed (0.1 m s^{-1}). For unreinforced 6061 Al and A356 Al alloys a transition from mild to severe wear occurred in the ranges 175–190 °C and 225–230 °C respectively. With the addition of 20 vol.% Al_2O_3 to 6061 Al, the mild to severe wear transition was raised to a range between 310–350 °C. Likewise, an addition of 20 vol.% SiC to the A356 Al increased this transition to 440–450 °C. A hybrid A356 Al composite containing 20 vol.% SiC and 10 vol.% graphite remained in a mild wear regime at the highest test temperature of 460 °C. All the reinforced alloys were able to withstand considerable thermal softening effects while remaining in a mild sliding wear regime. This is attributable to the formation of protective transfer layers of comminuted reinforcing particulates and transferred steel debris from slider counterfaces. Graphite in the hybrid composite introduced greater mild wear losses compared with the other composites due to increased friability and contact surface extrusion effects. The absence of severe wear phenomena in this composite contributes to the inhibition of comminution and fracture by graphite entrained in the surface tribolayer. [WIL 1996]

2.13 Interfaces

Interface between any two phases can be explained as bounding surface where a discontinuity of some kind occurs .The discontinuity may be sharp or gradual. In general the interface is essentially bidimensional region through which material parameters, such as concentration of an

element, crystal structure elastic modulus, density and coefficient of thermal expansion , change from one side to another . Thus bonding between two phases at interface is termed as interfacial bonding. In case of composites, bonding at particle – matrix interface is called interfacial bonding.

The behavior of a composite material is a result of combined behavior of the following :

1. Reinforcing element
2. Matrix
3. The interface between the fiber and matrix

2.14 Types of Bonding at the interface

It is important to be able to control the degree of bonding between matrix and the reinforcement .To do so , it is necessary to understand all the different possible bonding types, one or more of which may be acting at a given instant .We can conveniently classify the important types of interfacial bonding as follows

1. Mechanically bonding
2. Chemical bonding

a) Dissolution and wettability bonding

b) Reaction bonding

2.14.1 Mechanical bonding

Simple mechanical keying effects between two surfaces can lead to a considerable degree of bonding .Any contraction of the matrix onto a central fiber would result in a gripping of the later by the former .There has been some work on mettalics wires in the metal matrices indicating that in the presence of internal compressive forces , a wetting or metallurgical bond is not quite necessary because the mechanical gripping of fiber by the matrix is sufficient to cause an effective reinforcement as indicated by the occurrence of multiple necking in fibers .

2.14.2 Chemical bonding

There are two types of chemical bonding:

1. Dissolution and wettability bonding: In this case, interaction between components occurs at an electronic scale. Since this interaction is on short range it is important that components come into intimate contact on an atomic scale.

2. Reaction bonding: In this case, a transport of atoms occurs from one or both of components to reaction site, that is, the interface. This atomic transport is controlled by diffusional process .Two polymer surface may form a bond owing to the diffusion of matrix molecules to the molecular network of the fiber thus forming tangled molecular bonds at the interface .

2.15 Wettability between reinforcement and matrix alloy

Wettability can be defined as the ability of a liquid to spread on a solid surface. It also describes the extent of intimate contact between a liquid and a solid. Successful incorporation of solid ceramic particles into casting requires that the melt should wet the solid ceramic phase. The basic means used to improve wetting are

(a) Increasing the surface energies of the solid,

(b) Decreasing the surface tension of the liquid matrix alloy,

(c) Decreasing the solid-liquid interfacial energy at the particles-matrix

Several approaches have been taken to promote the wetting of the reinforcement particles with a molten matrix alloy, including the coating of the particles, the addition of alloying elements to the molten matrix alloy, the treatment of the particles, and ultrasonic irradiation of the melt. In general, the surface of non-metallic particles is not wetted by the metallic metal, regardless of the cleaning techniques carried out. Wetting has been achieved by coating with a wettable metal. Metal coating on ceramic particles increases the overall surface energy of the solid, and improves wetting by enhancing the contacting interface to metal-metal instead of metal-ceramic.

Nickel and copper are well wetted by many alloys, and have been used for a number of low melting alloys. In general, these coatings are applied for three purposes, viz., to protect the reinforcement from damage in handling, to improve wetting, and to improve dispensability before addition to the matrix. The type of coating, in terms of wettability, can be divided into coating which reacts with the matrix, and coating which reacts with the oxide layer of the metal.
Heat treatment of the particles before dispersion into the melt aids their transfer by causing desorption of adsorbed gases from the particle surface. Heating silicon carbide particles to 900°C, for example, assists in removing surface impurities and in the desorption of gases, and alters the surface composition by forming an oxide layer on the surface. Hence a clean surface provides a better opportunity for melt-particles interaction, and thus, enhances wetting. Thus results in strong interfacial bonding.

Cevdet Kaynak et.al. studied, the fatigue behaviour of aluminium matrix–silicon carbide (SiC) particulate reinforced composite in comparison to the matrix aluminium alloy containing 12 wt% Si. Three different weight percentages of SiC particulates: 5, 10, and 15 in the size range of 40–60 microns were injected into the melt. Mg was also added to improve the wettability of Al alloy matrix over SiC particulates resulting in better interfacial bonding. Test specimens were machined from squeeze casting billets.
Hardness, bending and fatigue tests indicated that reinforcing the Al-alloy matrix with SiC particulates improved the hardness, flexural strength and fatigue resistance with increasing content of SiC particulates. Stress levels yielding less than 107 cycles to fracture were applied. Cracks initiated at the debonded particulate–matrix interface and/or by the cracking of the coarse particulates. SiC particulates improved fatigue resistance mainly by acting as barriers to cracks and/or deflecting the growth plane of cracks resulting in decreased crack propagation rates.

Fig. 2.2 : Fractographs (a, b) showing adhesion at the interface between the Al-alloy matrix and SiC particulates

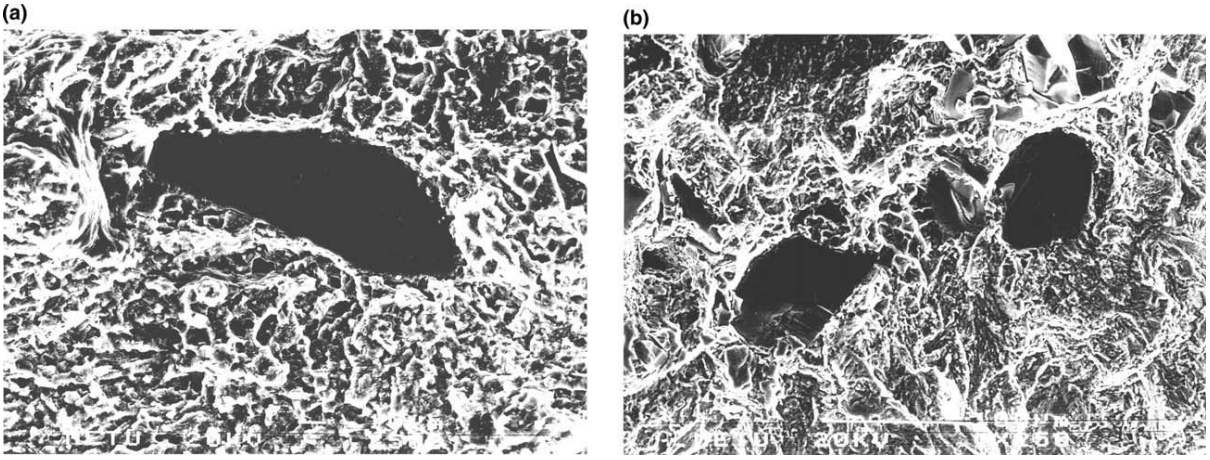

Fig.2.3: Crack initiation at SiC particles especially due to debonding at the interface under high stress levels

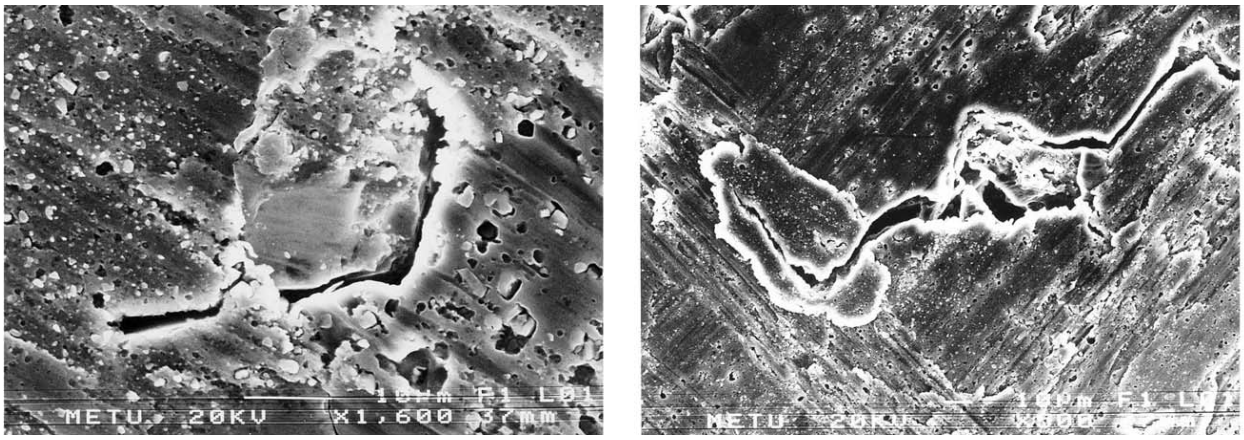

Hardness and flexural strength values increased as the weight fraction of SiCp increased. This is due to strain hardening in the regions surrounding the particles,due to the CTE mismatch between the matrix and the particulates resulting in a high dislocation density.

Conversely, flexural strain at fracture values decreased due to the decreased ductility. Mg addition during melting of the Al-alloy matrix improved the wettability resulting in certain bonding at the particulate-matrix interface. However, under higher stress levels the interfacial bond strength was not sufficient and cracks initiated at the debonded interface. Another crack

initiation mechanism was the fracture of SiCp especially seen in the specimens with coarse particulates. Fatigue striations were observed in the Al-alloy matrix during early crack growth and propagation periods [CEV 2006]

Stephane Pompidou studied condition of crack deviation on the basis of the mechanism that Cook and Gordon proposed for a combination of similar materials. Deviation results from debonding ahead of crack tip, as a result of a stress component operating perpendicular to interface. The condition can take into account the presence of an interphase and several interfaces. It leads to a master curve relating interface and uncracked constituent strengths to Young's moduli of constituents. The master curve was established using finite element computation of the stress state at crack tip in a cell of dissimilar materials separated by an interface, and considering the maximum of stress component perpendicular to interface. This maximum is obtained when crack tip is very close to the interface. This distance is equal to curvature at crack tip. The situation pertinent to crystalline materials was considered. As a consequence, the master curve provides an overestimation for non crystalline materials. The model can explain and predict crack deviation within an interphase with respect to strength of fibre/interphase bond. [STE 2007]

E. Ghassemieh studied the Composites with a weak interface between the filler and matrix which are susceptible to interfacial crack formation are studied. A finite-element model is developed to predict the stress/strain behaviour of particulate composites with an interfacial crack. Another case arises when there is no bonding between the inclusion and the matrix. In this latter case the slip boundary condition is imposed on the section of the interface which remains closed. The states of stress and displacement fields are obtained for both cases. The location of any further deformation through crazing or shear band formation is identified as the crack tip. A completely unbonded inclusion with partial slip at a section of the interface reduces the concentration of the stress at the crack tip. Whereas this might lead to slightly higher strength, it decreases the load transfer efficiency and stiffness of this type of composite. An interesting result of the present study is that besides matrix properties, deformation rate and temperature, the nature of the stress concentrating heterogeneities also determines the mode of tensile deformation; the bi-axial stress state induced by poorly adhering glass beads promotes ductile

shear deformation at the expense of brittle crazing. This insight may be of interest in the development of new composite materials. By avoiding a triaxial stress state at the stress concentrators, a ductile response to tensile deformation might be achieved under test conditions that otherwise would yield a brittle response. [GHA 2001]

A. Pramanik, L.C. Zhang investigated the deformation mechanisms of MMCs subjected to micro-indentation by a spherical indenter using a three dimensional finite element modeling. It was found that deformation behavior, hardness and work hardening of MMCs were highly dependant on the location of indentation relative to particles, volume percentage of the particle, and the size ratio of indenter to particle. The hardness of an MMC varied in a complex manner depending on the restriction on the matrix flow by reinforced particles and work hardening of the matrix material. Hardness increased with the increase of volume percentage of reinforced particles and decrease of the size ratio of indenter to particle. Matrix flow due to indentation was highly non-uniform which generated an inhomogeneous strain filed in an MMC.
Due to the presence of reinforcements, MMCs behave very differently compared to monolithic metals during deformation. While micro-indentation is simple to carryout, the test results at low indentation loads should be interpreted carefully because the microscopic deformation processes are complex. Following results were concluded:

(i) The ceramic particles increase the MMC's ability to resist deformation, but this is highly dependant on the location of indentation relative to particles, volume percentage of particles, size ratio of indenter to particle and applied load. Consequently, these parameters affect hardness of MMCs.
(ii) The mechanisms responsible for the anisotropy of MMCs are: varied restriction to matrix flow by particles and non-uniform work hardening of matrix material depending on the combination of above mentioned parameters.
(iii) The micro-indentation test under low load cannot give to a consistent measure of the hardness of MMCs.

These pose a question that the conventional definition of micro-hardness is not very appropriate for characterizing MMCs. [PRA 2007]

CHAPTER-3

EXPERIMENTAL WORK

3.1 Synthesis of Al-4.5wt%Cu/zircon sand/SiC Hybrid composite

Details of raw materials

A brief description of the raw materials used in the synthesis of composite is presented as follows:

3.1.1 Matrix material

Aluminum copper master alloy was prepared in a muffle furnace. Commercially pure aluminum was cut from its ingot size into smaller pieces by an electric power saw in order to feed the crucible properly. Aluminum was first melted at 720°C and then 30 wt% pure copper in wires form was dipped completely inside the aluminum melt. The melt was then covered by a flux (4NaCl + 1 KCl) to minimize loss due to oxidation.

Composition of master alloy was analyzed and the chemical composition of the master alloy is given in table 3.1

Table 3.1 – Chemical composition of master alloy

Element	Cu	Mg	Si	Fe	Mn	Al	Cr
Wt. %	16	0.03	0.13	0.30	0.01	83.52	0.01

Al-4.5wt% Cu alloy was then prepared from the master alloy (Al-16wt%Cu) by adding the calculated amount of aluminium to the master alloy that is required to make it Al-4.5wt% Cu alloy. This alloy is used as matrix material for the synthesized hybrid composite.

3.1.1.1 Chemical analysis

For chemical analysis, as-cast alloy was drilled and chips were collected from different parts of the ingot. Procedure for chemical analysis for estimation of Cu present in the cast alloy is as follows:

One gram sample was weighed and dissolved in boiling HCl. A little amount of concentrated HNO_3 acid was added, which fully dissolves aluminum and copper present in it. About 5ml of concentrated H_2SO_4 was added and stirred while being heated till it became paste. The paste was then cooled to room temperature and was re-dissolved in distill water. Adequate amount of NH_4OH was added followed by addition of acetic acid. The solution was cooled and potassium iodide (10g) was added and stirred, followed by the addition of starch indicator. The solution was titrated with $Na_2S_2O_3$ till it became colorless. Burette reading of $Na_2S_2O_3$ consumed was used to calculate the amount of copper in the alloy by the following formulae

$$\% \text{ Cu} = 0.0063 \times Na_2S_2O_3 \text{ consumed}$$

3.1.2 Reinforcement material

Zircon sand and silicon carbide was used as reinforcement material. Particle size of as received Zircon sand was in the range between 75-200 μm and for Silicon carbide it was 45–100 μm. The as received reinforcement particles were sieved and required particle size were selected as given in the table 3.2

Table 3.2 –Particle size range of zircon sand and Silicon Carbide

Reinforcement	Particle size range (μm)
Zircon sand	125 - 150
Silicon Carbide	51 - 90

Chemical composition of the zircon sand used in the present work is given in the table 3.3

Table 3.3 – Chemical composition of zircon sand

Component	ZrO_2	SiO_2	TiO_2	Fe_2O_3	Volatiles
Wt.%	65.30	32.80	0.27	0.12	1.51

3.2 Synthesis

A stir casting setup (Fig. 3.1), which consisted of a resistance furnace and a stirrer assembly, was used to synthesize the composite. The stirrer assembly consisted of a graphite turbine stirrer, which was connected to a variable speed direct current (D.C.) motor (speed 0 to 1700 rpm) by means of a steel shaft. The stirrer was made by cutting and shaping a graphite block to desired shape and size. The stirrer consisted of three blades at angles of 120° apart. Fig. 3.2 shows the photograph of the stirrer from two different angles. Clay graphite crucible of 1.5 Kg Al melt capacity was placed inside the furnace. Top pouring arrangement was made to cast the composite in metal mould. The stirrer assembly consisted of a graphite turbine stirrer fixed to a steel rod. Approximately 700gms of alloy was then remelted at 820°C in the resistance furnace of stir casting setup. Preheating of zircon sand and silicon carbide mixture at 450°C was done in a resistance furnace, placed near stir casting setup, to remove moisture and gases from the surface of the particulates. The stirrer was then lowered vertically up to 3 cm from the bottom of the crucible (total height of the melt was 9 cm). The speed of the stirrer was gradually raised to 700 rpm and the preheated zircon sand and silicon carbide was added with a spoon at the rate of 10-20g/min into the melt. The speed controller maintained a constant speed, as the stirrer speed got reduced by 50-60 rpm due to the increase in viscosity of the melt when particulates were added into the melt. After the addition of zircon sand, stirring was continued for 10 minutes for better distribution. The melt was kept in the crucible for one minute in static condition and it was then top poured in two small metal moulds (3cm×3cm×11cm) and (dia 1.5 cm × length 10 cm) Fig. 3.3 successively .

Fig. 3.1 –Stir casting set-up

Fig. 3.2 - Graphite turbine stirrer

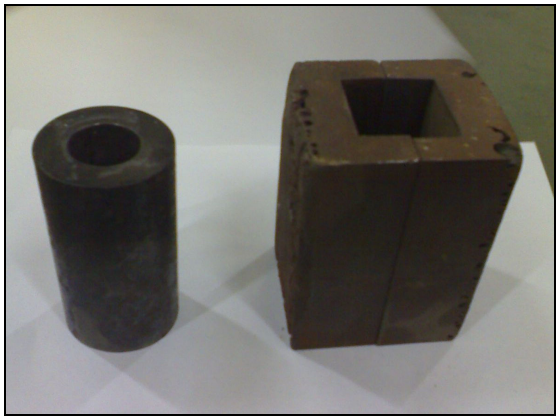

Fig. 3.3 –Metal Moulds

Table 3.4 - As cast aluminum based hybrid composites

Matrix alloy	***Particulate reinforcement***	***Average particle size (µm)***	***Vol %***
Al-4.5wt% Cu	Zircon sand + Silicon carbide	Z = 135, S = 65	Z = 10, S =5

3.3 Characterization

Particles distribution was evaluated with the help of optical microscope and image analyzer. XRD studies were carried out to confirm the presence of various reinforcements in the alloy matrix. Scanning electron microscopy of the composite was studied and with the help of X ray dot mapping and with EDS facilities the distribution of individual reinforcements were examined.

3.4 Study of interfacial bonding with help of microhardness testor

Interfacial bonding in the as cast hybrid composite was examined with the help of microhardness testor (Fig.3.4). By taking indentations with varying loads 100 gm, 200gm , 300gm on the selected particle, hardness of the particle was calculated .Different set of readings were made by varying the different parameters like time (10 sec, 15 sec, 20 sec and 25 sec) , load (100 gm, 200 gm, 300 gm) etc. Particles were assigned as P(1) , P(2), P(3) and so on.

Fig. 3.4 –Microhardness testor

CHAPTER-4

Results and Discussions

4.1 Synthesis of Al-4.5wt%Cu/zircon sand/SiC Hybrid composite

Important process parameters for synthesizing the hybrid composite by stir casting process are stirrer design and position, stirring speed and time, melting and pouring temperature, particle-preheating temperature, particle incorporation rate, mould type and size, and reinforcement particle size and amount. These parameters are discussed in the following sections.

4.1.1 Stirrer design

Stirrer design is an important factor in stir casting process as it is responsible for vortex formation and uniform distribution of reinforcements. Different designs and material for designing stirrers are available but stirrer made out of graphite is more durable compared to metallic stirrers. For better machining of stirrer, fine grain graphite material with control machining is required. Graphite stirrer is generally used in the shape of flat blade due to the difficulty in machining. Hence a graphite turbine stirrer has been designed which is more durable and effective in particle dispersion compared to other stirrers (Fig. 3.2). It is experimentally found that steel stirrer gets damaged only after 1-2 melting process where as graphite stirrer lasts upto 12-13 melting. In the case of zircon sand dispersion in aluminium alloy (Al-4.5wt%Cu), the mulling action of graphite turbine stirrer is found to be very effective for uniform distribution of particles.

4.1.2 Stirrer position

It has been experimentally found that effective vortex is formed at 700 rpm when the stirrer is at 1/3 of the melt height from the bottom. It is observed that if the height is more than 1/3 of the melt height from the bottom, a small ineffective vortex is formed, which results in insufficient dispersion of reinforcement particles. Also, if the height is less than 1/3 of the melt height from

the bottom, the vortex disappears and particle dispersion is stopped. In the present study, the approx. height of melt in the crucible is kept at 9 cm from the bottom and stirrer height is kept 3 cm from the bottom. Thus an effective vortex is formed which results in the sufficient dispersion of reinforcement particles. According to the experimental observation the stirrer should be placed at a height which is no more than 30% from the base to avoid accumulation of particles at the bottom of the mixture.

4.1.3 Stirring speed and time

A mechanical force can usually be used to overcome surface tension to improve wettability. The stirring speed has been raised upto a constant speed of 700 rpm as it is the maximum speed in which smooth vortex is formed without melt turbulence and spattering. It is experimentally found that when stirring speed is less than 700 rpm, ineffective vortex is formed that leads to non dispersion of particles in the aluminium melt. When the stirring speed is raised to 800 rpm, there is turbulence and spattering of melt. Stirring time depends upon the amount of reinforcement particles to be dispersed in aluminium alloy melt. After complete addition of zircon sand and silicon carbide, stirring has been continued for 10 minutes for better distribution.

4.1.4 Melt temperature

Melt temperature is kept at 780-800ºC as the increase in reinforcement particles amount increase the melt viscosity, which hinder stirring speed. It is experimentally found that the melt temperature of 780-800ºC is suitable for controlling the stirring speed and effective dispersion. Moreover, the optimum temperature of Al-alloy melt for the dispersion of particles is found to be in the range of 740-800ºC [Ban 1983]. As the temperature falls below 700ºC, viscosity of the melt increases and hence after the addition of reinforcement particles viscosity increases too much and results in the solidification of melt. If the temperature is kept above 800^0C the viscosity of melt reduces too much that results in the settling of particles in the melt without dispersing in the melt during stirring.

4.1.5 Particle size and amount

It is observed that particle size and amount affects the synthesis process of hybrid composite. When the particle size is very less (< 50 μm), it results in agglomeration either at the bottom or top of melt in the crucible. It is observed that if particle size is too much small, particles tends to float on the surface of melt. Fine particles have a tendency to agglomerate during synthesis, when added above a certain amount, depending upon its size. These agglomerates entrap air and there is a decrease in their density. A combined effect of decrease in density, buoyant force of the melt and stirring action results in a floatation of these agglomerates on liquid melt during synthesis. Larger particle size (> 200 μm) results in the non dispersion of particles and settling of particles at the bottom of crucible. It is observed that particles are rejected from the melt when the added amount is more than 20wt%. Hence, in the present experimental conditions it is not possible to synthesize composites reinforced with particles of weight fraction over 20wt%.

4.1.6 Particle preheating temperature

The zircon particles and silicon carbide particles have been preheated at 450ºC to remove moisture and gases from the surface of the particulates. If moisture and gases will be there then the chances of agglomeration will be there due to the presence of entrapped air in the particles. The Preheating furnace is kept close to the stir casting set up to avoid drop in temperature of zircon particles during transporting particles from preheating furnace to stir casting set-up.

4.1.7 Particle incorporation rate

It is observed from the experimental data (table 4.3) that a good dispersion is achieved when PIR is less (10-20 gm/min). Dispersion of particles reduces significantly when PIR is 30-40 gm/min. High PIR leads to agglomeration of particles followed by rejection from the alloy melt. It is observed that there is no dispersion of particles for PIR above 40 gm/min. In such high rate (>40 gm/min) particles settles at the bottom of the crucible without getting wetted by the liquid alloy. The decrease in particle dispersion with increased PIR is due to the agglomeration of the particles at the top of the melt. The agglomerates are difficult to wet by aluminium melt and

hence they tend to settle at the bottom. During particle incorporation, particle free fall in the melt is more important so that particles can disperse uniformly in the melt.

Table 4.1 - Dispersion of particles in Al-4.5wt%Cu alloy for different PIR.

Particle incorporation rate (g/m)	Observation
10-20	Good dispersion
30-40	Poor dispersion / Agglomeration
> 40	Particle rejection

4.2 Microstructural characterization

Particles distribution was evaluated with the help of Optical micrography and Scanning electron microscopy. Results of the study are as follows:

4.2.1 Optical micrography

Fig.4.1 shows the optical micrographs of as cast hybrid composite .It is observed from fig. (a) & (b) that the particles are uniformly distributed through the matrix. Fig. (c) & (d) shows the optical micrographs of hybrid composite at higher magnifications. It is observed that there is a strong interfacial bonding between particles and matrix as there are no visible traces of any porosity and inclusions in the interfacial regions. Zircon sand and silicon carbide particles are difficult to distinguish by optical micrography .So for this purpose SEM is carried out.

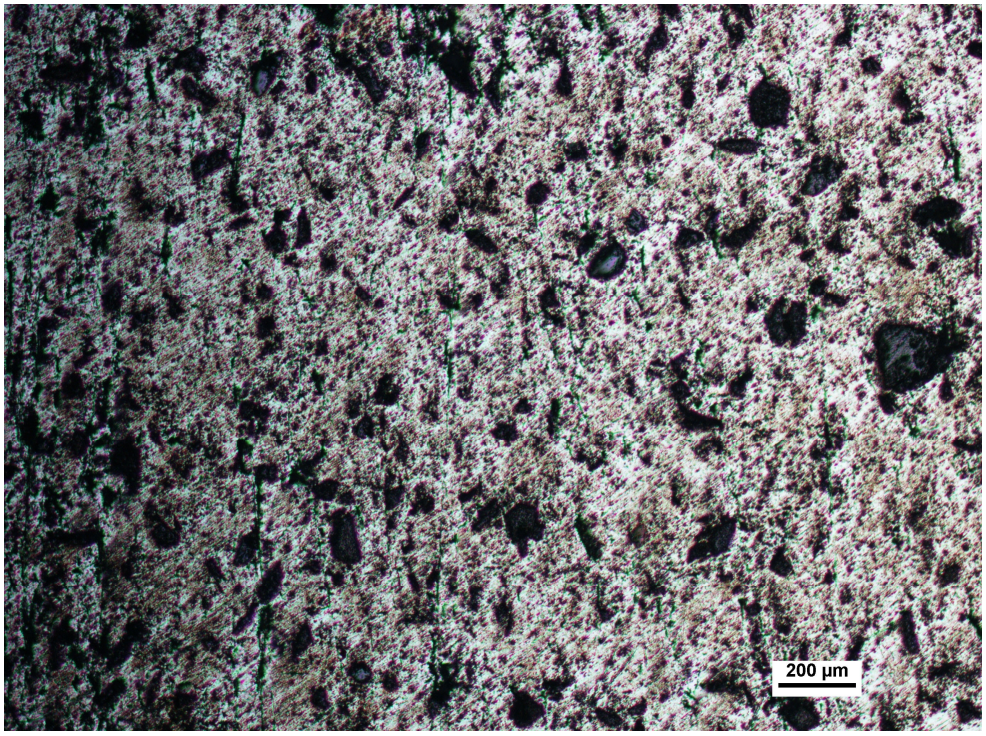

(a)

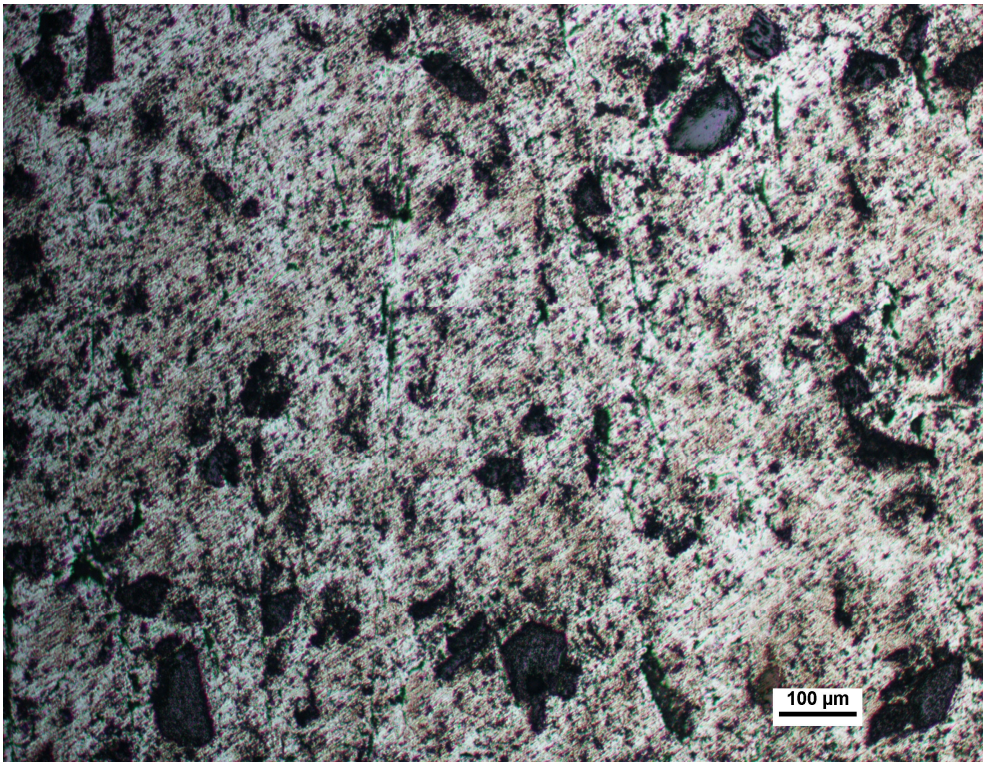

(b)

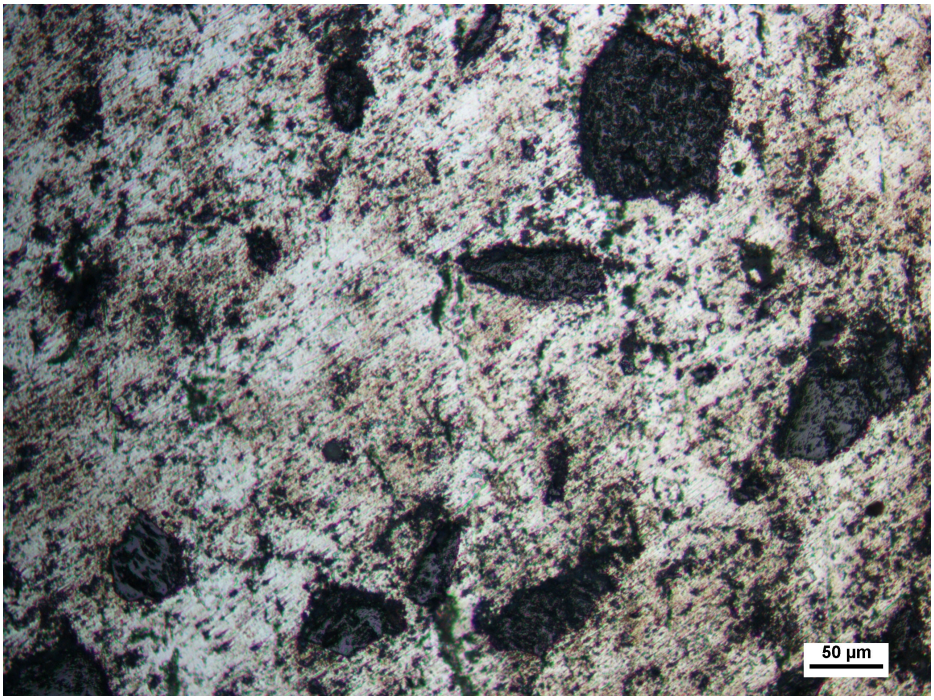

(c)

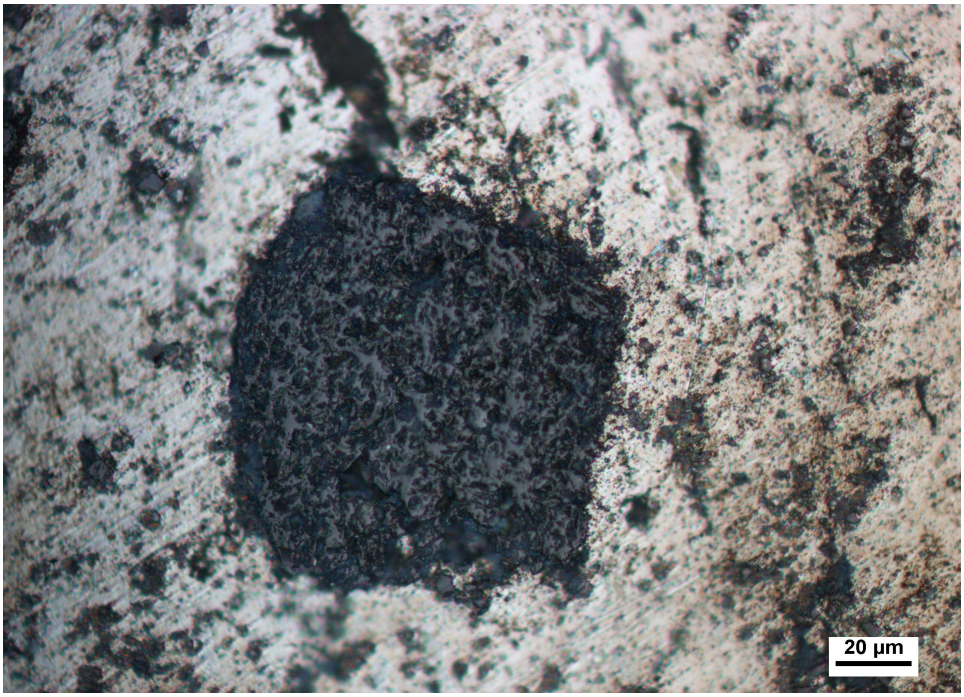

(d)

Fig 4.1 – Optical micrographs of Hybrid composite a) 50X, b) 100X, c) 200X, d) 500X

4.2.2 Scanning electron microscopy

Fig. 4.2 shows the scanning electron micrographs of the hybrid composite. It is observed that the particles are uniformly distributed throughout the matrix for the cast hybrid composite. Agglomeration of particles in some regions is clearly visible; this is due to the presence of porosity associated to it. Presence of entrapped air and moisture in the reinforcement particles results in the porosity after casting.

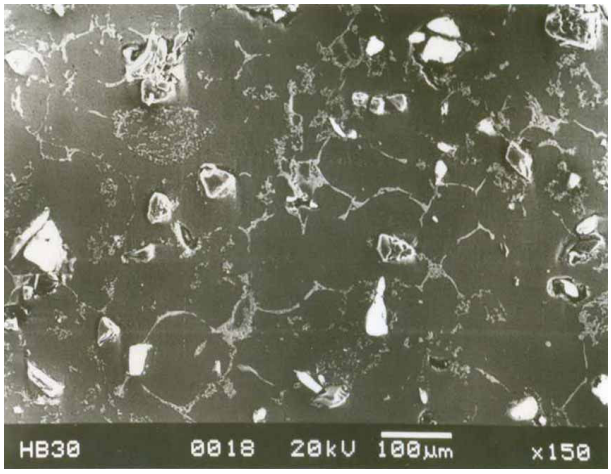

Fig 4.2 Scanning electron micrograph of hybrid composite

Fig 4.3 shows the scanning electron micrograph of hybrid composite at higher magnification. The different particle types are clearly visible in this micrograph. Two different types of particle are visible in these micrographs. But still it is not possible to distinguish zircon sand and silicon carbide particles.

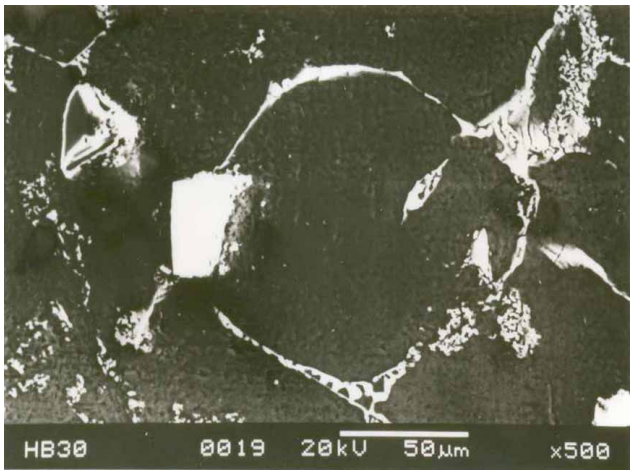

Fig. 4.3 – Scanning electron micrograph of hybrid composite at higher magnification

Fig. 4.4 shows X-ray dot map of the microstructure. It is observed that the bright particle is rich in Zr and Si, whereas dark particle is rich in Si. This indicates the presence of zircon sand as well as silicon carbide particle in the hybrid composite

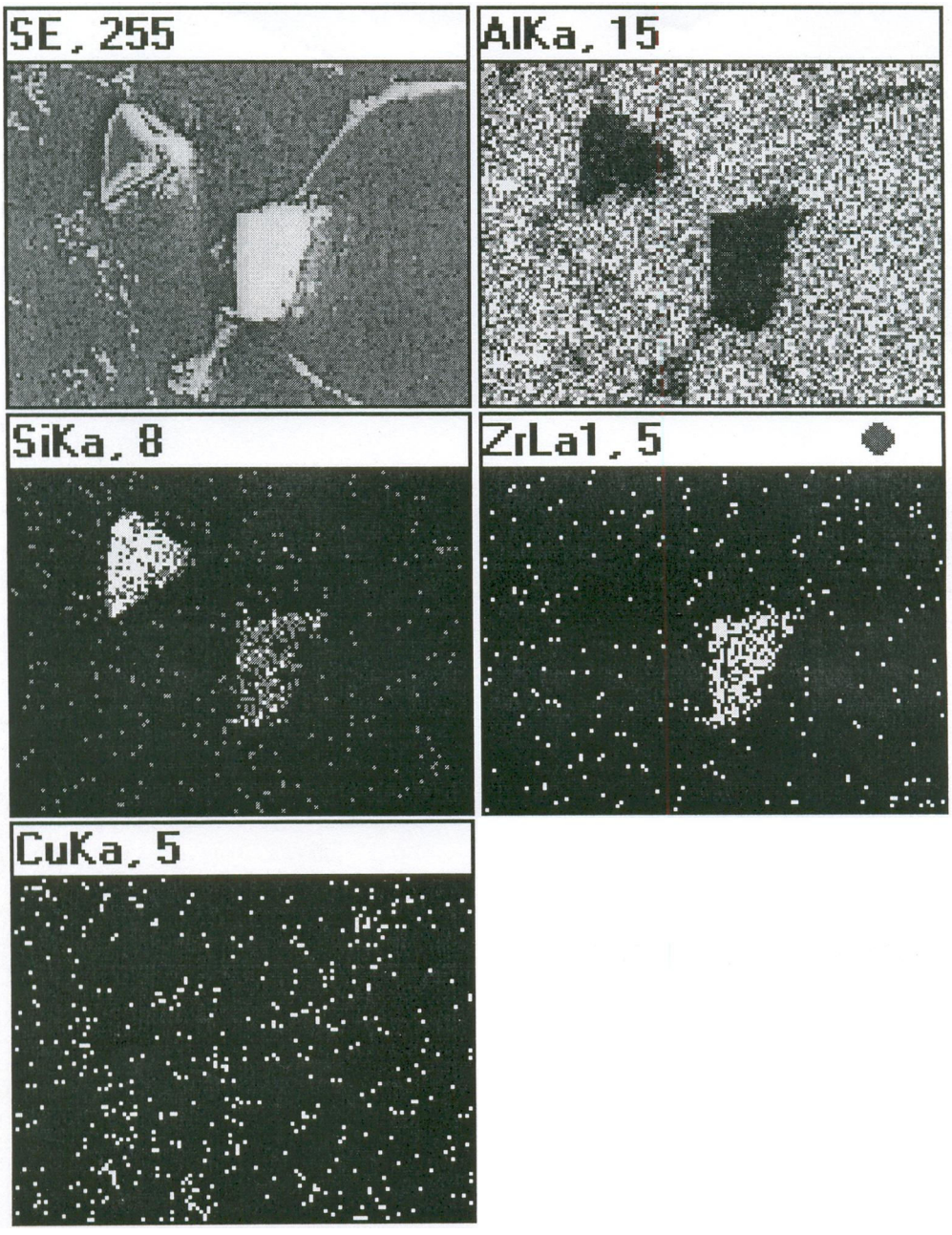

Fig. 4.4 – X-ray dot map of hybrid composite

Fig. 4.5 shows the X-ray diffraction pattern of the hybrid composite, which show the presence of Al, SiC, $ZrSiO_4$ and $CuAl_2$. This confirms the presence of zircon sand as well as silicon carbide particle in the cast hybrid composite. Hence, it is confirmed that dark and bright particles in hybrid composite microstructures are silicon carbide and zircon sand, respectively.

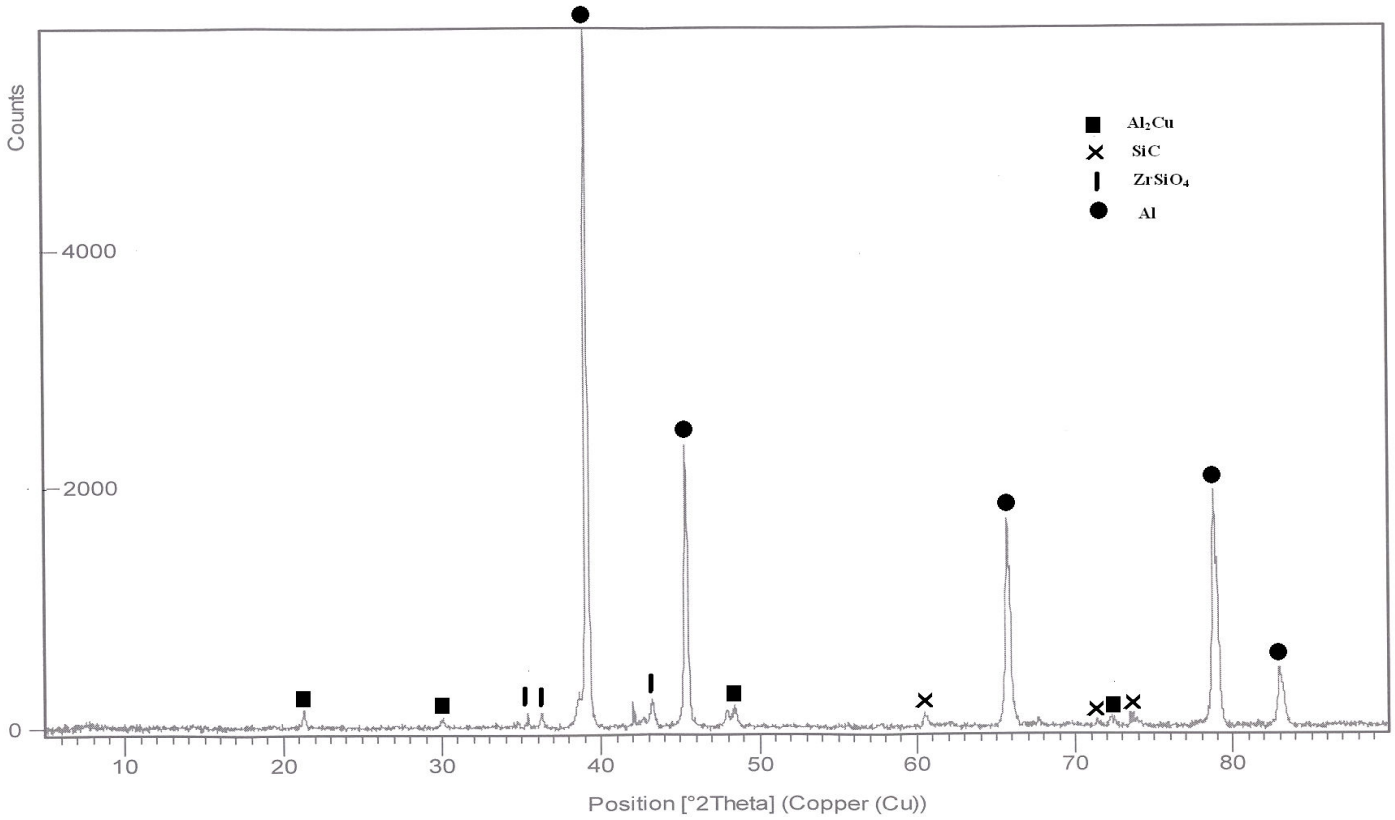

Fig. 4.5 –X-ray diffraction pattern of the hybrid composite

4.3 Microhardness of the particles dispersed in the Al-4.5wt%Cu matrix

In this section microhardness of zircon sand and silicon carbide particles is studied by varying the parameters like indentation time 10sec, 15sec, 20sec, 25sec and the indentation load 100gm, 200gm, 300gm. Fig.4.6 shows the optical micrograph of hybrid composite, Indentations at indentation load 300 gm and 200 gm are clearly visible in this micrograph .Indentation size at load 300 gm is bigger than that of indentation load 200 gm.

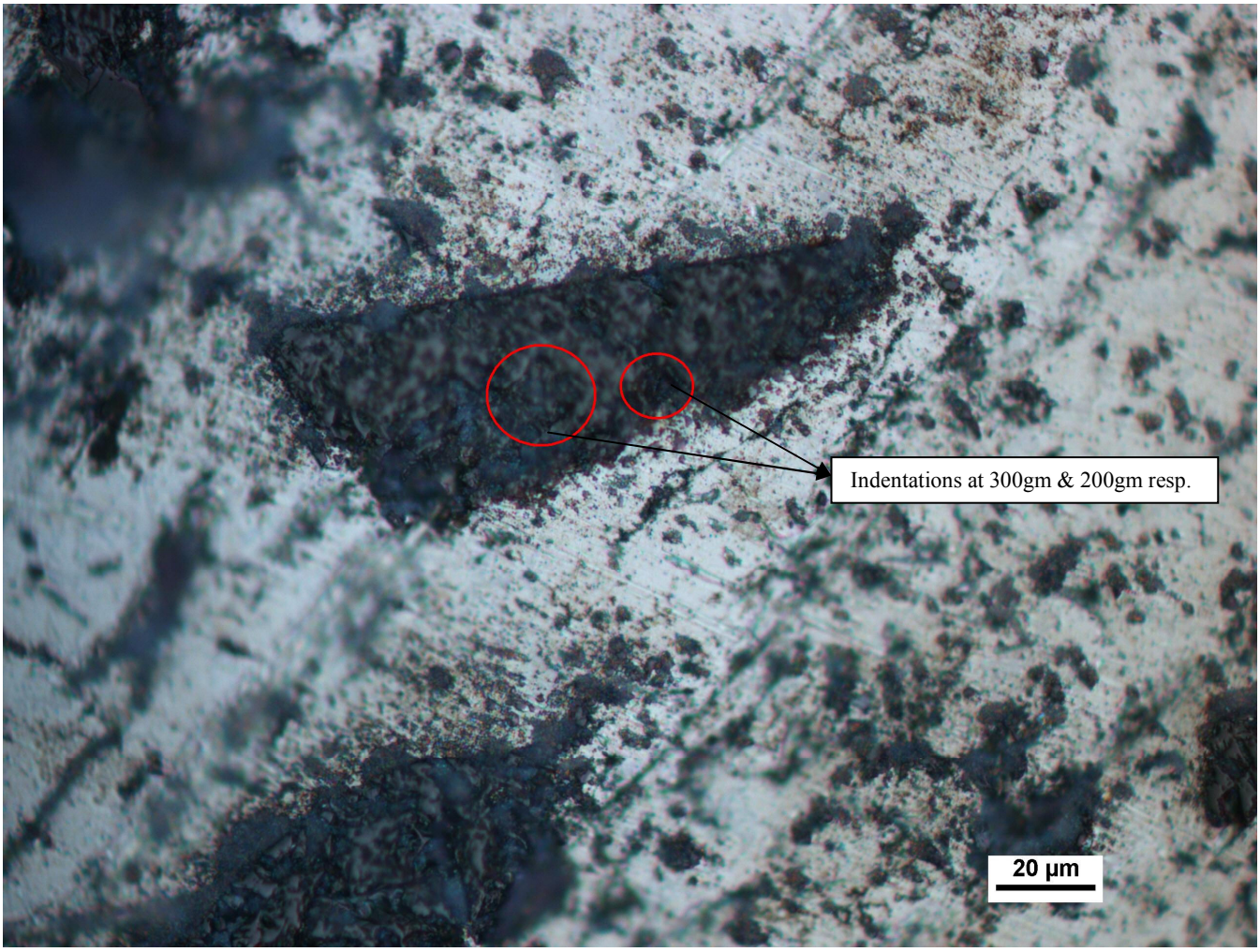

Fig.4.6 Optical micrograph at 500X, showing microindentations

4.3.1 Variation of microhardness of zircon sand particles with indentation load

Fig.4.7 shows the variation of microhardness of zircon sand particles with varying indentation loads 100gm, 200gm & 300gm for indentation time 10 sec. It is observed that micro indentations under load 100 gm does not shows the consistent values of hardness. This shows 100gm load is insufficient to give the exact values of particle hardness. In the case of 200gm and 300gm indentation loads, consistent hardness values are observed. It is clear from the fig.4.7 for particle P(1), Hv200 > Hv300, it can be attributed to the weak interfacial bonding. If the interfacial bonding is poor, particle tends to slip down at the indentation load 200gm and thus gives more microhardness value than the actual. For particle P(3) Hv300 > Hv200, here indentation load 200gm is insufficient to let the particle to slip from its position and when the indentation load 300gm is applied particle slips down from its position and gives the hardness value which is more than the actual one. Thus a weak interfacial bonding is observed at matrix – zircon particle interface for some particles ie. P(1), P(2), P(10).

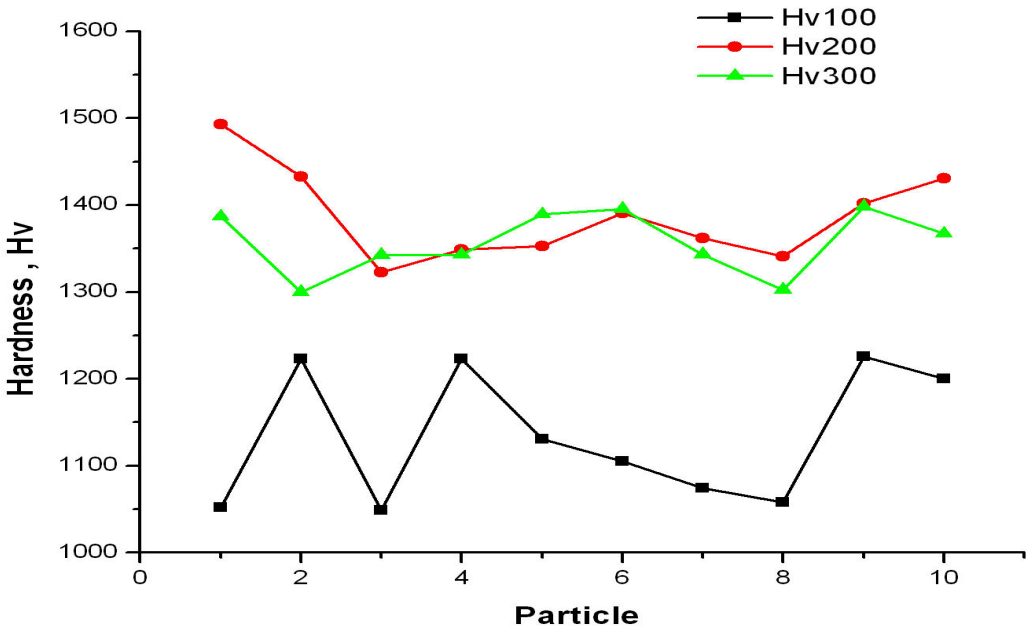

Fig.4.7 –Variation of microhardness of zircon sand particles with varying indentation loads for indentation time 10 sec

Table 4.2- Microhardness of Zircon particles for indentation time 10 sec

Particle	Hv100	Hv200	Hv300
1	1052.24	1493.05	1386.72
2	1223.11	1432.74	1300
3	1048.62	1322.56	1342.35
4	1223.11	1348.88	1342.88
5	1130.55	1352.5	1389.31
6	1105.18	1390.45	1395.38
7	1073.95	1362	1343
8	1057.62	1340.86	1302.55
9	1225.3	1402.05	1398.11
10	1200.15	1430.65	1367.06

Fig.4.8 shows the variation of microhardness of zircon sand particles with varying indentation loads for indentation time 15 sec. Again it is observed that indentation load 100gm is insufficient to give exact values of hardness. In the case of 200gm and 300gm indentation loads, consistent hardness values are observed. It is clear from the fig.4.8 that Hv200 ≈ Hv300 for all particles. Thus a strong interfacial bonding is observed at matrix – zircon particle interface.

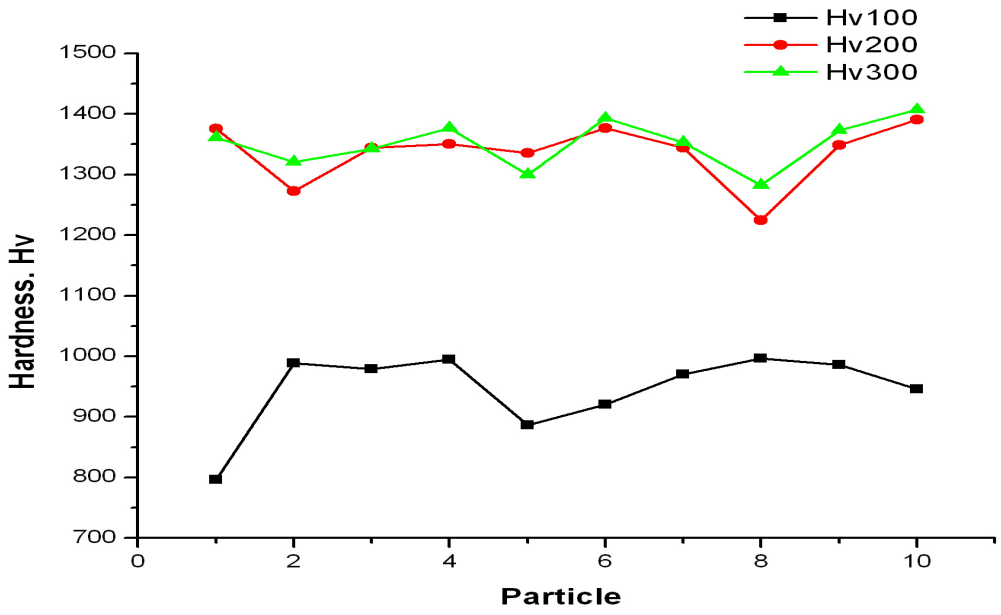

Fig.4.8 –Variation of microhardness of zircon sand particles with varying indentation loads for indentation time 15 sec

Table 4.3 – Microhardness of Zircon particles for indentation time 15 sec

Particle	Hv100	Hv200	Hv300
1	796.39	1375.8	1361.13
2	988.96	1272.18	1321
3	978.63	1344	1342.75
4	994.73	1350.15	1376.92
5	886.5	1335.17	1300
6	920.17	1376.89	1392.95
7	970	1344	1353
8	996.39	1224.63	1282.33
9	985.9	1348.19	1373.15
10	946	1390.17	1407.15

Fig.4.9 shows the variation of microhardness of zircon sand particles with varying indentation loads for indentation time 20 sec. As explained in the previous sections, it can be attributed from the fig. 4.9 that for the particles P(5) & P(10) weak interfacial bonding is observed at matrix – zircon particle interface.

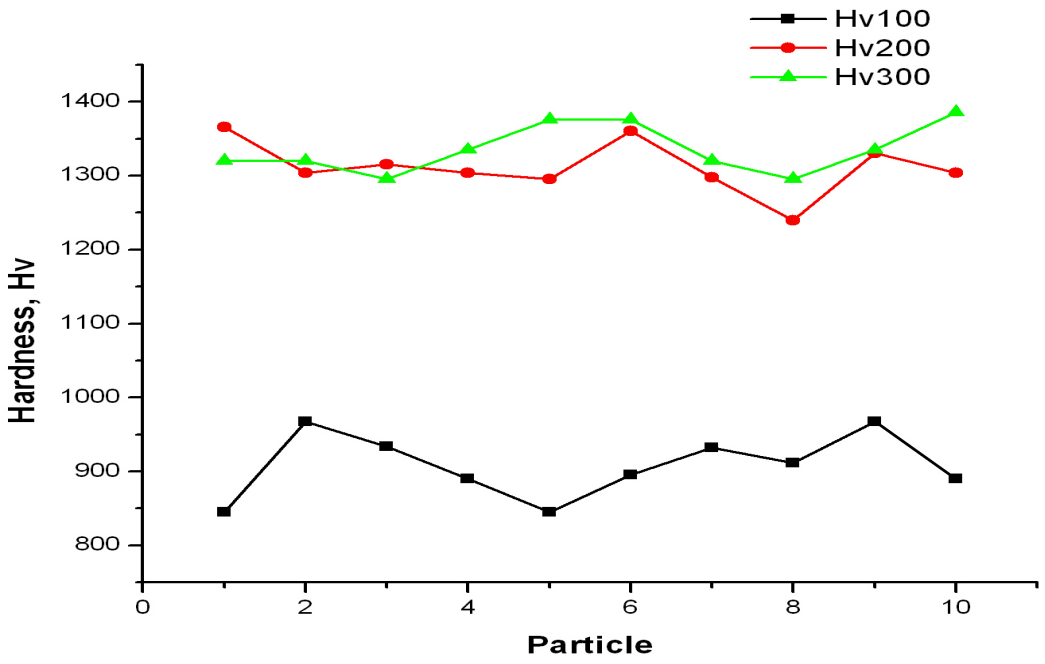

Fig.4.9 –Variation of microhardness of zircon sand particle with varying indentation loads for indentation time 20 sec

Table 4.4 - Microhardness of the Zircon particles for indentation time 20 sec

Particle	Hv100	Hv200	Hv300
1	845.23	1366	1320.05
2	967.23	1304.12	1320.05
3	933.65	1315	1295.45
4	889.85	1304.12	1335
5	845	1295.35	1375.65
6	895.19	1360.08	1375.65
7	932	1297.45	1320.05
8	911.15	1239.77	1295.45
9	967.15	1330.45	1335
10	889.85	1304.12	1385.68

Fig.4.10 shows the variation of microhardness of zircon sand particles with varying indentation loads for indentation time 25 sec, As explained in the previous sections, it can be attributed from the fig. 4.10 that for the particles P(1), P(5), P(6), P(9) & P(10) weak interfacial bonding is observed at matrix – zircon particle interface.

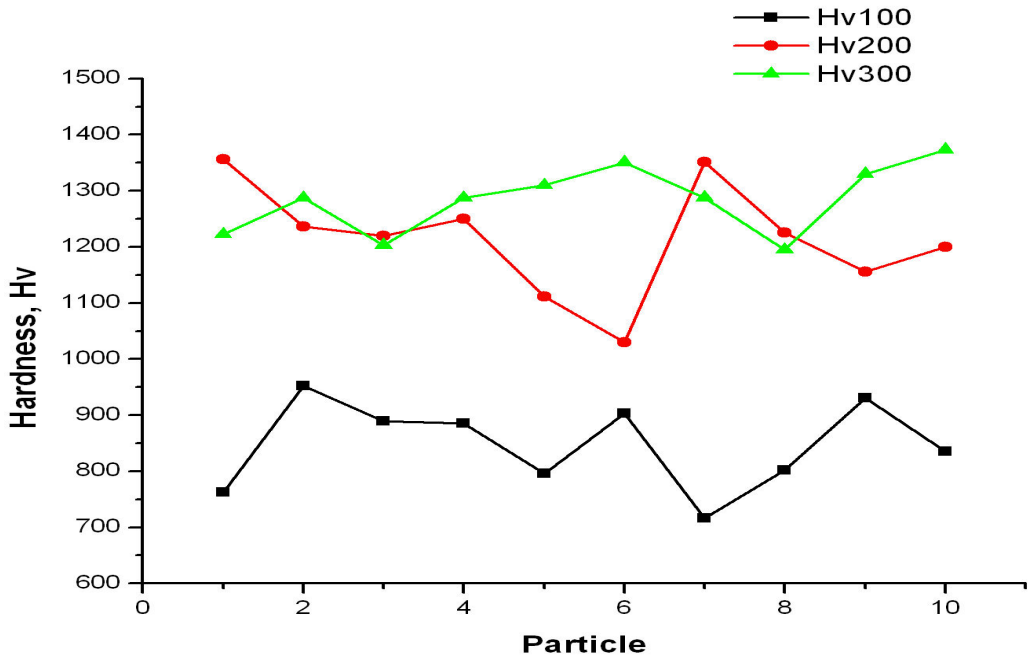

Fig.4.10 –Variation of microhardness of zircon sand particles with varying indentation loads for indentation time 25 sec

Table 4.5 - Microhardness of the Zircon particles for indentation time 25 sec

Particle	Hv100	Hv200	Hv300
1	762.41	1355.95	1222.45
2	952.38	1236	1287.09
3	888.88	1220	1203.35
4	885.07	1250	1287
5	795.5	1111.85	1310
6	903	1030	1350.75
7	715.9	1350.85	1287.9
8	802	1225	1195
9	930.15	1155.55	1330
10	835.15	1200	1373

Hence it is concluded that when microhardness values are studied for the same indentation time and for varying indentation loads i.e., 100 gm, 200 gm, 300 gm. Micro indentations under load 100 gm does not give consistent measure of hardness. So 100gm load is insufficient to give the exact values of particle hardness. For indentation loads 200 gm and 300 gm significant results are observed. By conventional definition of microhardness, Microhardness should be a constant value for different indentation loads. But in the present study different microhardnes values are there for different indentation loads i.e. 200 gm and 300 gm, due to the weak interfacial bonding in the case of few particles.

4.3.2 Variation of microhardness of zircon particles with time

Fig.4.11 shows the variation of microhardness of zircon sand particles with same indentation load 100 gm and varying indentation time .It is observed that Hv100, 10 sec > Hv100, 15 sec > Hv100, 20 sec > Hv100, 25 sec. It can be explained on the basis of fact that if the interfacial bonding is strong then with the increase in indentation time, diagonal of indentation increases. Thus microhardness decreases with the increase in indentation time and indentation diameter as indentation diameter is related to the microhardness by the following relation

$$Hv = 1.854 \times P/d^2$$

$$Hv \alpha 1/d^2$$

Where , P is the applied load

d is the diagonal length of indentation

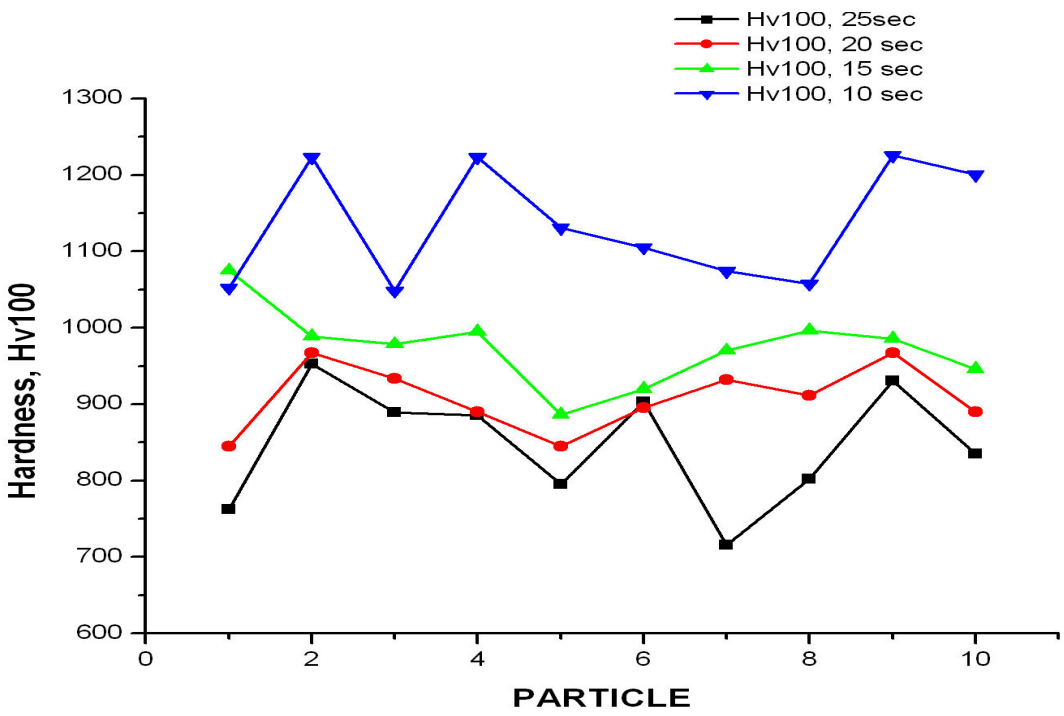

Fig.4.11 –Variation of microhardness of zircon sand particles with same indentation load 100 gm and varying indentation time

Table 4.6 –Microhardness of the zircon particles at indentation load=100 gm, for different indentation time

Particle	Hv100, 25 sec	Hv100 , 20 sec	Hv100 ,15 sec	Hv100 , 10 sec
1	762.41	845.23	1075	1052.24
2	952.38	967.23	988.96	1223.11
3	888.88	933.65	978.63	1048.62
4	885.07	889.85	994.73	1223.11
5	795.5	845	886.5	1130.55
6	903	895.19	920.17	1105.18
7	715.9	932	970	1073.95
8	802	911.15	996.39	1057.62
9	930.15	967.15	985.9	1225.3
10	835.15	889.85	946	1200.15

Fig.4.12 shows the variation of microhardness of zircon sand particles with same indentation load 200 gm and varying indentation time, similar results are observed as in fig.4.10 with the slight variation in microhardness values at few particles .The reason for this is the variation in the weak interfacial bonding and strong interfacial bonding at different particle – matrix interfaces .

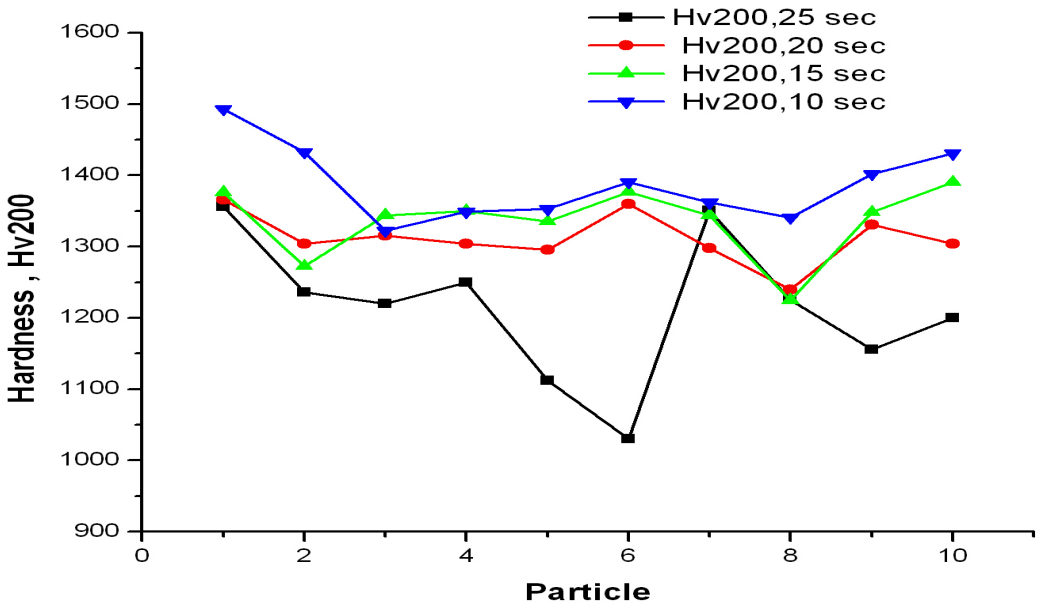

Fig.4.12 –Variation of microhardness of zircon sand particle with same indentation load 200 gm and varying indentation time

Table 4.7 –Microhardness of the Zircon particles at indentation load=200 gm, for different indentation time

Particle	Hv200, 25 sec	Hv200 , 20 sec	Hv200, 15 sec	Hv200 ,10 sec
1	1355.95	1366	1375.8	1493.05
2	1236	1304.12	1272.18	1432.74
3	1220	1315	1344	1322.56
4	1250	1304.12	1350.15	1348.88
5	1111.85	1295.35	1335.17	1352.5
6	1030	1360.08	1376.89	1390.45
7	1350.85	1297.45	1344	1362
8	1225	1239.77	1224.63	1340.86
9	1155.55	1330.45	1348.19	1402.05
10	1200	1304.12	1390.17	1430.65

Fig.4.13 shows the variation of microhardness of zircon sand particles with same indentation load 300 gm and varying indentation time again similar results are observed as discussed in the fig. 4.12

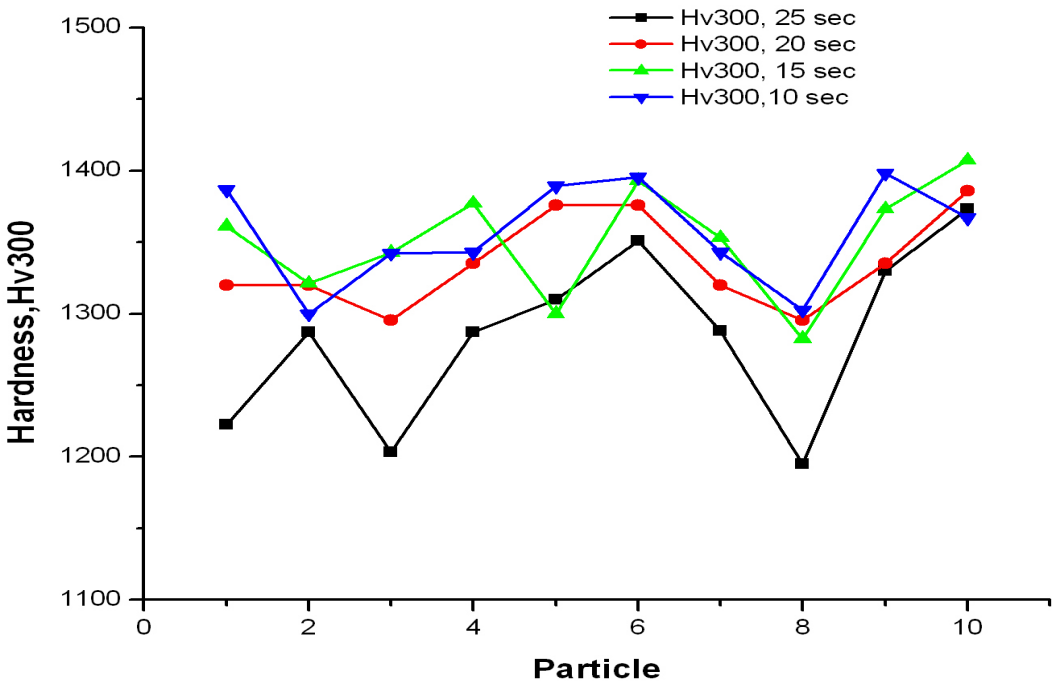

Fig.4.13 –Variation of microhardness of zircon sand particles with same indentation load 300 gm and varying indentation time

Table 4.8 –Microhardness of the Zircon particles at indentation load=300 gm , for different indentation time

Particle	Hv300, 25 sec	Hv300, 20 sec	Hv300 ,15 sec	Hv300, 10 sec
1	1222.45	1320.05	1361.13	1386.72
2	1287.09	1320.05	1321	1300
3	1203.35	1295.45	1342.75	1342.35
4	1287	1335	1376.92	1342.88
5	1310	1375.65	1300	1389.31
6	1350.75	1375.65	1392.95	1395.38
7	1287.9	1320.05	1353	1343
8	1195	1295.45	1282.33	1302.55
9	1330	1335	1373.15	1398.11
10	1373	1385.68	1407.15	1367.06

4.3.3 Variation of microhardness of Silicon carbide particles with indentation load

Fig.4.14 shows the variation of microhardness of SiC particles with varying indentation loads for indentation time 10 sec. It is observed that micro indentations under load 100 gm does not shows the consistent values of hardness as in the case of zircon particles. So 100gm load is insufficient to give the exact values of particle hardness. In the case of indentation loads 200gm and 300gm consistent values of hardness are there. It is clear from fig. 4.14, approx. for all particles Hv200 = Hv300. Thus it can be attributed that a strong interfacial bonding exists at matrix (Al-4.5wt%Cu) - reinforcement (SiC) interface.

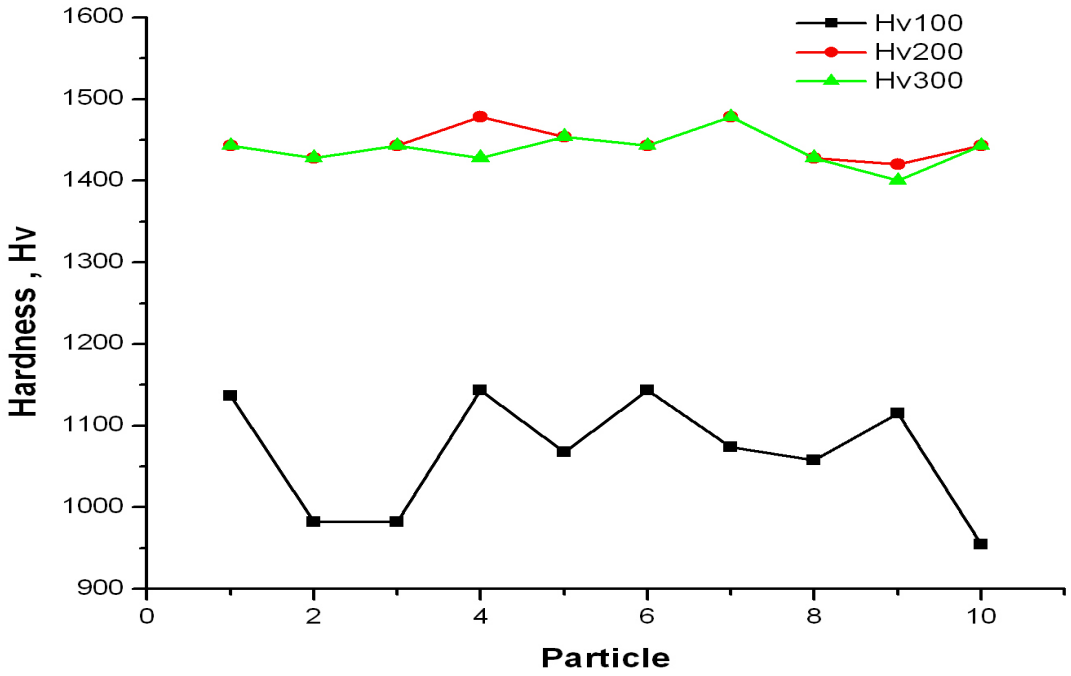

Fig.4.14 - Variation of microhardness of SiC particles with varying indentation loads for indentation time 10 sec

Table 4.9 - Microhardness of the Silicon carbide particles for indentation time 10 sec

Particle	Hv100	Hv200	Hv300
1	1136.65	1443	1443
2	982	1428	1428
3	982	1443	1443
4	1143.5	1478	1428
5	1067.34	1454	1454
6	1143.5	1443	1443
7	1073.95	1478	1478
8	1057.62	1428	1428
9	1115.3	1420	1400
10	954.43	1443	1443

Fig.4.15 shows the variation of microhardness of SiC particles with varying indentation loads for indentation time 15 sec. Same trend of microhardness values are there as observed in the fig.4.14

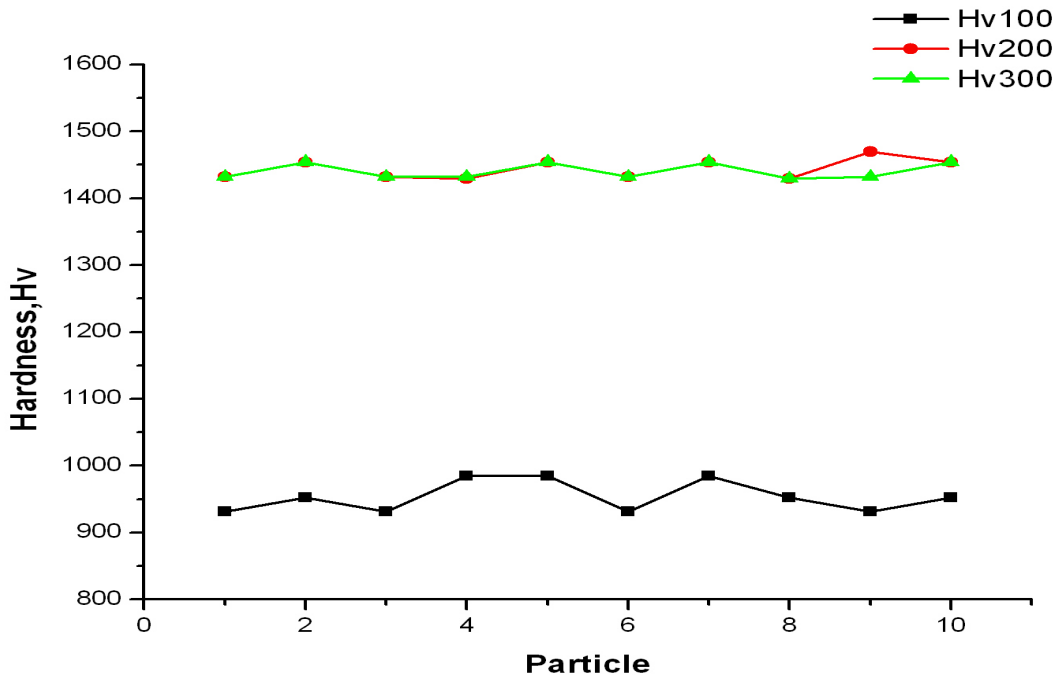

Fig.4.15 Variation of microhardness of SiC particles with varying indentation loads for indentation time 15 sec

Table 4.10 - Microhardness of the Silicon carbide particles for indentation time 15 sec

Particle	Hv100	Hv200	Hv300
1	931	1432	1432
2	952	1454	1454
3	931	1432	1432
4	985	1429	1432
5	985	1454	1454
6	931	1432	1432
7	985	1454	1454
8	952	1429	1429
9	931	1470	1432
10	952	1454	1454

Fig.4.16 shows the variation of microhardness of SiC particles with varying indentation loads for indentation time 20 sec. It is again observed that microindentations under load 100 gm does not give consistent measure of hardness values as in the case of zircon particles. So 100gm load is insufficient to give the exact values of particle hardness. For indentation loads 200gm and 300gm, Hv200 = Hv300 (for approx. all particles).

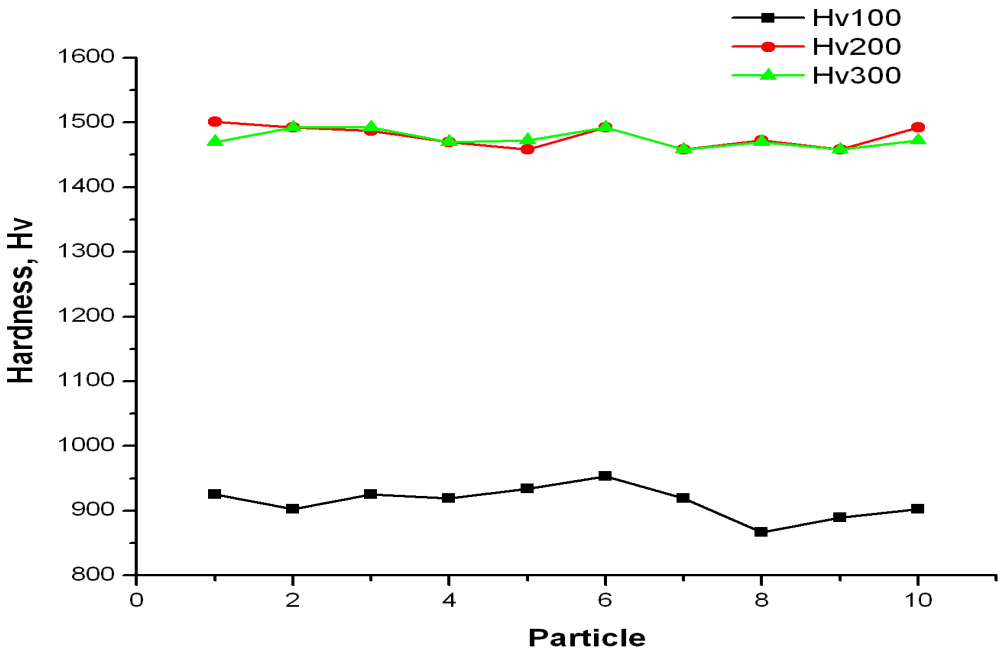

Fig.4.16 - Variation of microhardness of SiC particles with varying indentation loads for indentation time 20 sec

Table 4.11 - Microhardness of the Silicon carbide particles for indentation time 20 sec

Particle	*Hv100*	*Hv200*	*Hv300*
1	925	1501	1470
2	902.5	1492	1492
3	925	1487.34	1492
4	919.24	1470	1470
5	933.67	1458	1472.45
6	953	1492	1492
7	919.24	1458	1458
8	867	1472.45	1470
9	889.78	1458	1458
10	902.5	1492	1472

It can be concluded that by micro hardness tester we can determine the interfacial bonding between the matrix and reinforcement particles. In the present investigation SiC particles show excellent interfacial bonding .It can be attributed to interfacial reaction between SiC and Al-4.5 wt% Cu alloy, which enhances the interfacial bonding .But in case of zircon particle few particle were not bonded perfectly with the matrix. It can be attributed to the fact that zircon sand does not react with Al-4.5 wt% Cu alloy matrix and hence mechanical bonding (which may be weak during synthesis process) is predominately on chemical bonding.

CHAPTER - 5

CONCLUSIONS

The following conclusions can be drawn from the present investigation:

1. Al-4.5 wt% Cu alloy matrix composites reinforced with zircon particles and silicon carbide particles can be successfully synthesized by the stir casting method.

2. For synthesizing of hybrid composite by stir casting process, stirrer design and position, stirring speed and time, melting and pouring temperature, particle-preheating temperature, particle incorporation rate, mould type and size, and reinforcement particle size and amount are the important process parameters.

3. Microstructural observations shows that the zircon particles are uniformly distributed in the Al-4.5 wt% Cu alloy matrix and good interfacial bonding between reinforcing particles and matrix.

4. The micro-indentation test under low load cannot give to a consistent measure of the particles hardness in hybrid composite.

5. For the hybrid composites at higher loads, microhardness values at a particular indentation load decreases with the increase in indentation time. If the matrix - particle interfacial bonding is strong then microhardness values will be same for varying indentation loads. If the matrix - particle interfacial bonding is weak then the indentation diagonal is comparatively small than actual.

6. Al-4.5wt%Cu as matrix has strong interfacial bonding with SiC particles than that of zircon sand particles.

REFERENCES

[DAS 2007] Sanjeev Das, Siddhartha Das, Karabi Das, Composites Science and Technology 67 (2007) 746–751

[STE 2007] Ste´phane Pompidou , Jacques Lamon , Composites Science and Technology 67 (2007) 2052–2060

[MAI 2007] Maik Thu¨nemann, Olivier Beffort , Simon Kleiner, Ulrich Vogt, Composites Science and Technology 67 (2007) 2377–2383

[RKU 2007] R.K.Uyyuru.M.K.Surappa,S.Brusethaug ,tribology international 40(2007)365-373

[PRA 2007] A. Pramanik, L.C. Zhang , J.A. Arsecularatne, Composites Science and Technology 68 (2008) 1304–1312

[HAY 2006] Hayrettin Ahlatci, Tolga Kocer, Ercan Candan, C. Huseyin, Tribology International 39 (2006) 213.

[HUB 2006] T. Huber, H.P. Degischer , G. Lefranc , T. Schmitt, Composites Science and Technology 66 (2006) 2206–2217

[NAT 2006] N. Natarajan , S. Vijayarangan , I. Rajendran ,Wear behaviour of A356/25SiCp aluminium matrix composites sliding against automobile friction material. Wear 261 (2006) 812–822

[OLI 2006] Olivier Beffort, Siyuan Long, Cyril Cayron, Jakob Kuebler, Philippe-Andre´ Buffat Composites Science and Technology 67 (2007) 737–745

[CEV 2006] Cevdet Kaynak , Suha Boylu, Materials and Design 27 (2006) 776–782

[JIN 2004] Jinhai Gu, Xiaonong Zhang, Mingyuan Gu, Min Gu, Xike Wang, Journal of Alloys & Compounds 372 (2004) 304.

[JIN 2004x] Jinhai Gu, Xiaonong Zhang, Mingyuan Gu, Xike Wang, Journal of Alloys & Compounds .

[FER 2004] Ferhat Gul , Mehmet Acilar , Composites Science and Technology 64 (2004) 1959–1970

[HUI 2004] Hui-Hui Fu, Kyung-Seop Han, Jung-Il Song, Wear 256 (2004) 705.

[WUJ 2003] Wu Jiejun, Li Chenggong, Wang Dianbin, Gui Manchang, Composites Science and Technology 63 (2003) 569–574

[RSC 2003] R.Schaller,Alloys Compd. 355 (2003) 131

[NAI 2003] S.M.L. Nai, M. Gupta, C.Y.H. Lim Composites Science and Technology 63 (2003) 1895–1909

[WEI 2002] J. N. Wei, H. F. Cheng, Y. F. Zhang, F. S. Han, Z. C. Zhou and J. P. Shui, *Materials Science and Engineering A*, *Volume 325, Issues 1-2*, *28 February 2002*, *Pages 444-453*

[MAN 2001] Manchang Gui and Suk Bong Kang *Materials Letters*, *Volume 51, Issue 5*, *December 2001*, *Pages 396-401*

[GHA 2001] E. Ghassemieh, Composites Science and Technology 62 (2002) 67–82

[SHA 1999] S. C. Sharma, B. M. Girish, D. R. Somashekar, Rathnakar Kamath, B. M. Satish, Composites Science and Technology, 59 (1999) 180

[TDP 1998] T.P.D. Rajan, R. M.Pillai, B. C.Pai; Journal of Material Science, 33, (1998) 3491.

[SUR 1997] M. K. Surappa, J. Mater. Proc. Tech. 63 (1997) 325.

[WIL 1996] S. Wilson and A. T. Alpas *Wear*, *Volume 196, Issues 1-2*, *August 1996*, *Pages 270-278*

[SON1995] J. I. Song, H. D. Bong and K. S. Han, Suipta Metallurgica et materialia, 33 (1995) 1307.

[RJP 1993] R.J Perez, J. Zhang, R.J Gungor, MetallMater.Trans.A 24 (1993)701

[JHA 1994] J.Zhang ,R.J.Perez, E.J.Lavernia, Acta. Matall. Mater . 42 (1994) 395

[JHA 1993] J.Zhang ,R.J.Perez, E.J.Lavernia,J.Mater.Sci. 28 (1993) 2395

[LEE 1992] Lee CS, Kim YH, Han KS, Lim T. Wear behaviour of aluminium matrix composite materials. J Mater Sci 1992;27:793–800.

[SRI 1991] T. S. Srivatsan, I. A. Ibrahim, F. A. Mohamed, E. J. Lavernia; Journal of Material Science, 26 (1991) 5965.

[GEI 1989] A. L. Geiger, M. Jackson, Adv. Mater. Process, 7 (1989) 23.

[RAC 1988] H.J. Rack, Dispersion Strengthened Aluminum Alloys, Ed. By Y.W. Kim and W.M. Griffith, p.649, The Minerals, Metal and Materials Society (1988).

[MOH 1988] W. R. Mohn, D. Vukobratovich, J. Mat. Eng., 10 (1988) 225

[JOH 1987] W. S. Johnson, ASTM Standardization News, Oct., 1987, 36-39.

[BAN 1983] A. Banerji, M. K. Surappa and P. K. Rohatgi, *Metall. Trans. B*, 14B (1983) 273.

[HOS 1982] Hosking FM, Folgar Portillo F, Wonderlin R, Mehrabian R. Composite of aluminium alloys: fabrication and wear behaviour. J Mater Sci 1982;17:477–98.

[ENG1966] Engineering properties of selected ceramic materials, Battelle Memorial Institute (The American Ceramic Society, Ohio, 1966).